HIFI AOT Release Notes v2.0

I. Point, Map, Spectral Scan AOTs: DBS Modes

Released 08/03/2010

II. Point AOT: Position Switch, Frequency Switch, Load Chop Modes

Released 06/04/2010

Abstract

This document summarizes the readiness of the HIFI Observing Modes for PSP/SDP/RP observing, based on analysis of AOT testmode observations and engineering tests carried out over the Performance Verification phase on redundant HIFI subsystems.

Document: ICC/2010-009
Version 2.0 of 07/04/2010
56 pages

Document approval

Prepared by:	P. Morris
Checked by:	M. Olberg, V. Ossenkopf
Authorized by:	P. Roelfsema, R. Shipman

Distribution

ESA	Herschel Science Centre
HIFI steering committee	F. Helmich P. Roelfsema R. Shipman T. Phillips E. Caux J. Stutzki X. Tielens
HIFI Project Office	F. Flederus
HIFI Calibration Group	
HIFI ICC	
HIFI Key Programme Teams	

Revision history

Version	Date	Changes	Author
Draft	24/02/2010	First version for AOT readiness review with HSC.	PM
1.0	08/03/2010	Updates and revisions with HIFI ICC inputs	PM
1.1	05/04/2010	Merged DBS and Point non-DBS mode release notes	PM
1.2	07/04/2010	Integrated inputs from calibration team: A. Boogert, C. Borys, W. Jellema, C. McCoey, F. Herpin, J. Braine, S. Lord, V. Ossenkopf, M. Olberg, D. Teyssier, C. Risacher, I. Avruch	PM
2.0	10/04/2010	Minor edits, updates to noise figure M. Olberg, Tsys figures D. Teyssier. Release version to HSC.	PM

Contents

1. Preface and Acknowledgements

The special circumstances of HIFI's switch to redundant side operations and resuming with a compressed Performance Verification phase and accelerated Observing Mode release has been supported by not only the core group of HIFI Calibration Scientists and Instrument Engineers over the "long haul", but also the KP team apprentices who have been variously present at the HIFI ICC in the Fall of 2009 and during PV-II starting end-January 2010, and also the HIFI software development team who have been available at all times. AOT test planning has been done in consultation with the KP PIs coordinated by X. Tielens, Instrument P.I. F. Helmich, Project Manager P. Roelfsema, and with the Mission Scientist J. Cernicharo. These persons should be acknowledged, as having directly supported the flight qualification of HIFI as a science instrument.

AOT/Uplink Engineering Team:
P. Morris (Caltech), M. Olberg (SRON/Chalmers), V. Ossenkopf (U. Köln), C. Risacher (SRON), D. Teyssier (HSC/ESA).

Instrument Engineers and System Architects:
P. Dieleman (SRON), K. Edwards (SRON), W. Jellema (SRON), A. de Jonge (SRON), W. Laauwen (SRON), J. Pearson (JPL).

HIFI Calibration Scientists:
I. Avruch (Kapteyn/SRON), A. Boogert (Caltech), C. Borys (Caltech), J. Braine (U. Bordeaux), F. Herpin (U. Bordeaux), R. Higgins (U. Maynooth), S. Lord (Caltech), T. Marston (HSC/ESA) C. McCoey (U. Waterloo), R. Moreno (Obs. Paris), M. Rengel (MPS)

HIFI Software Development Team:
R. Assendorp (SRON), B. Delforge (SRON), A. Hoac (Caltech), D. Kester (SRON), A. Lorenzani (Obs. Acetri), M. Melchior (U. Appl. Sci. NW Switzerland),W. Salomons (SRON), B. Thomas (SRON), E. Sanchez (CSIC), R. Shipman (SRON), Y. Poelman (SRON), J. Xie (Caltech), P. Zaal (SRON)

HIFI KP student/postdoc visitors:
E. DeBeck (U. Leuven), T. Bell (Caltech), N. Crockett (U. Michigan), P. Bjerkeli (Chalmers), P. Hily-Blant (Obs. Grenoble), M. Kama (U. Amsterdam), T. Kaminski (CAMK), B. Larsson (Obs. Stockholm), B. Lefloch (Obs. Grenoble), R. Lombaert (U. Leuven), M. de Luca (Obs. Paris), Z. Makai (U. Köln), M. Marseille (SRON), Z. Nagy (Kapteyn), Y. Okada (U. Köln), S. Pacheco (Obs. Grenoble), D. Rabois (U. Toulouse), Frank Schlöder (U. Köln), S. Wang (U. Michigan), M. van der Wiel (Kapteyn/SRON), M. Yabaki (U. Köln), U. Yildiz (U. Leiden)

HIFI KP PI Representatives to the ICC/AOT Team:
E. Caux (U. Toulouse), E. van Dishoek (U. Leiden), M. Gerin (Obs. Grenoble)

2. Introduction

The HIFI **Dual Beam Switch observing modes have been released in each of the Point, Mapping, and Spectral Scan AOTs** for carrying out PSP/SDP/RP observations starting February 28, 2010. Remaining **Point AOT observing modes, i.e. Position Switch, Frequency Switch (with and without sky reference), and Load Chop (with and without sky reference)** have been released for scheduling AORs using these modes starting in Cycle 12 (starting April 29), possibly in the latter part of Cycle 11 (starting April 8). This note summarizes the important performance aspects and caveats, as they are understood at the beginning of the first block of HIFI PSP observations. The audience for this note is the HIFI Users and Herschel Science Centre.

The results presented and discussed below have been obtained using the HIFI pipeline and tools available in the operational HCSS 2.X track (2.0 through 2.6), with the intention for Users to be able to reduce PSP data and reproduce results consistently with the version of the SPG at HSC. In some applications, only jython scripts are currently available (e.g., data cleaning and interactive baseline fitting), and certain tools in CLASS have been tested and used with observations exported from the HCSS to CLASS FITS.

Since the HIFI PSP scheduling overlaps with HIFI PV and there are many calibration observations still to be carried out and analyzed, and not all of the current results are understood, it is expected that this note will be updated.

3. Summary of Caveats and Conditions on Mode Release

3.1 DBS Observing Modes (Point, Map, and SScan AOTs)

All of the DBS modes and options they are offered in HSpot are released in all LO bands for science scheduling, with following exception and recommendations:

- **AORs which employ DBSCross and FastDBSCross maps are on hold** due to a command timing issue in uplink that can manifest itself in the pipeline as an asyncronicity of the ON/OFF phases and turn emission lines into absorption lines (or vice versa). The data quality is generally unaffected, and the problem is not systematic, but identification and workaround of the phase switch in the pipeline is not straightforward (to correct those affected observations), and has to be solved in the AOT logic.

- The initial results from comparing performances of the normal (or slow) chop DBS with FastDBS modes indicate that the latter generally perform better with respect to correction for electrical standing waves in Bands 6 and 7. This will be explained further below. **The recommendation at this time is to only use FastDBS in the HEB bands.**

3.2 Frequency Switch (Point AOT)

The Frequency Switch mode is released for SIS Bands 1-5. **This mode is not recommended in HEB Bands 6 and 7**, due to indications of poor stability in terms of baseline shapes, ripples, and artefacts that may not be treatable in IA such that S/N goals set by the User in HSpot can ever be achieved, and may thus compromise the intended science goals. **At this time, the recommendation is to use the alternative Load Chop mode in the HEB bands**.

It must be acknowledged that results leading to this recommendation are based on very few FSwitch testmode observations carried out in PV, mainly due to the limited AOT test time allowed for the HEB bands (effectively commencing only mid-way though PV-II) and the strong initial emphasis in PV-II on the DBS modes. Therefore the tradeoffs between FSwitch and LChop are not yet thoroughly studied. The few cases which have been studied (described more below) do exhibit less than nominal qualities, and thus the mode poses unacceptable risk to science given any of several contributing factors which have been known since TB/TV and early flight measurements, including difficult LO stabilization, very short Allan times, and occasional unstable pairings of the reference measurements after retuning when mixer currents are drifting.

This mode is also recommended to be used only with the sky reference option to obtain a spectrum at some User-selected line-free region (within 2 degrees of the science target) for standing wave correction in the pipeline. This is especially true for the diplexer Bands 3 and 4, in which the standing waves are not well-fit by one or two sine waves of constant amplitude. Only if the User expects very strong lines and is not concerned by the standing wave pattern in the surrounding baseline, or expects to be able to fit out the standing waves in IA when the lines are narrow, should the “no reference” option be considered.

3.3 Load Chop (Point AOT)

The Load Chop mode is released in all LO bands. Like the FSwitch mode, **LChop is recommended to be used only with the sky reference option** to obtain a spectrum at some User-selected line-free region (within 2 degrees of the science target) for standing wave correction in the pipeline, applying most strongly to Bands 3, 4, 6, and 7, and/or in cases where lines may be too broad for interactive ripple fitting.

3.4 Position Switch (Point AOT)

The PSwitch mode is release for all LO bands. No caveats on designed usage are currently needed.

3.5 Non-AOT mode specific

- LO signal purity
  - **Band 5b is not released for PSP-I or PSP-II**, due to signal purity issues that lead contamination from frequencies which are not part of the commanded tuning. Mapping observations in 5b done on CO (11-10) to verify pointing calibrations showed no CO line although the neighbouring transitions (in other bands) were easily detected. This points to a purity problem around those LO frequencies around 1261GHz, but may also apply to other frequencies in that band.
  - Similarly, Band 7a shows evidence of impurities when the LO is tuned in the range of 1755 – 1759 GHz. **AORs which request a fixed tuning over this range in 7a are on hold, and Spectral Scan AORs which scan through this range should be split into two AORs to avoid these frequencies.** When the region has been purified, the fixed point AORs can be released, and this region can be filled in for the Spectral Scans if desired (in consultation with the Helpdesk).
  - Several other frequencies or frequency ranges are suspect to contain unwanted LO signals, summarized in Sec. 4.

4. Spectral Purity

There are several frequencies in HIFI where the Local Oscillator has been shown to produce more than one frequency. In these cases, an observed spectrum will have some or all of the features from a different unknown (and possibly unstable) other frequency. When this is the case the mixer gain at the desired frequency will be unknown and it will not usually be possible to calibrate the flux accurately. Most of the impure regions were fixed in the ILT, TV/TB and CoP test campaigns; however, several frequencies remain to be addressed or cannot be addressed due to hardware safety considerations. The known impure frequencies include:

- **Band 3b**: LO frequencies near (±1 GHz) 941 and 952 GHz.
- **Band 4b**: LO frequencies above 1114 GHz (extreme upper end of tuning range).
- **Band 5a**: LO frequencies near (±2 GHz) 1135 GHz and (±2 GHz) 1206 GHz.
- **Band 5b** contains a number of frequencies covering a good fraction of the band. The full extent remains unknown so this band is currently unusable and was not included in the AOT release.
- **Band 7a:** LO frequencies between 1755 and 1759 GHz.
- **Band7b:** Currently there are no known remaining purity issues, but as a consequence of the some of the engineering adaptations needed to recover the purity and in some cases improve the stability of the system, there are

limitations in the robustness of the LO tuning in band 7b for observations targeting the C+ line. Fine characterization of the noise performances in this frequency range indicates that the mixer can be easily pumped up to 1897 GHz. Above this frequency, there is less LO power available but a decent pump level can be achieved until 1898 GHz. Above 1898 GHz, a regime is entered where the tuning of the mixer is less robust and is not always guaranteed to succeed. This means that, depending on the chain thermalization history, and on the exact targeted LO frequency, there can be observations which will suffer from very high system noise temperatures, usually rendering the scientific data very difficult to exploit.

The scheduling implications are summarized as follows:

- Spectral Scans in Bands 3b, 4b and 5a may be carried out as is, and Users should inspect and possibly discard the spectra taken at unruly the LO frequencies. This will imply some noise degradation after the spectrum deconvolution. (Note: 5b is not concerned by this recommendation as it is currently not yet considered releasable).

- For Spectral Scans in Band 7a, the User is advised to split the frequency coverage into at least two AORs which avoid the impure areas. As a consequence there will be a slight penalty due to the slew time tax charged at each AOR, and the (temporary) degradation of the achieved noise at the edges of the deconvolved spectra due to a coarser redundancy. Once the LO purity has been satisfactorily established, the excluded regions can be scanned if needed. Presently this means that LO tunings only over the following ranges are advised:

    - Band 7a: [1701.2 – 1755] and [1759 – 1793.8] GHz

  [Note: Several SDP and PSP1 AORs in Band 7a have been carried out over the impure ranges, prior to the preparation of this Release Note].

- For observations in Band 7b requesting LO frequencies > 1898 GHz, there are currently no scheduling restrictions, but Users must be aware of the lower performances that can result from the tuning issues described above.

- For single frequencies (in AORs using the Point and Map AOTs) whenever possible, the main lines of interest should be moved into the image bands if the new LO frequency falls in an area not affected by purity issues. Otherwise, it is probably wise to put the observations on hold until the chain is fixed in the targeted frequency area.

[Note: this will not have been possible for the very early SDP and PSP1 AORs which had to be scheduled prior to the preparation of this Release Note].

5. Noise performances

5.1 Fixed LO observations

HSpot provides noise estimates on a single sideband (SSB) main-beam brightness scale for combined H and V polarization spectra. Observations carried out in PV-II were analysed in order to verify these predictions, which drive observing time at goal and maximum spectral resolutions entered in HSpot by the User. The 1 GHz reference option has almost always been used in the noise predictions, which means that the baseline in only one WBS sub-band is considered for stability instead of the full IF, to take standing waves within that 1 GHz window into account. This is recommended for most observing situations except, when lines are very broad (such as from external galaxies or fast outflows).

Figure 1 shows the ratios of observed over predicted noise, at the goal and maximum spectral resolutions (entered in the AORs).

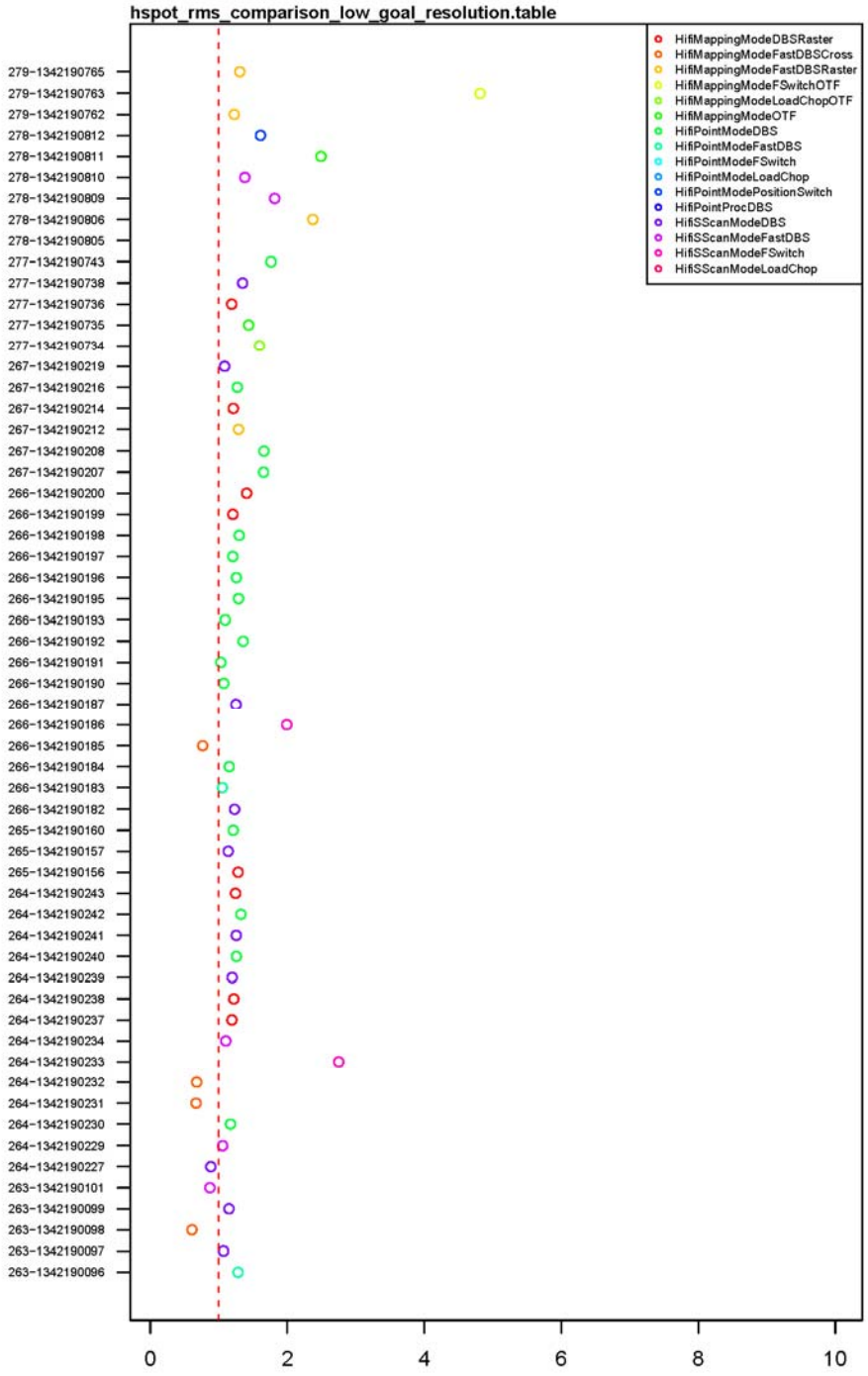
hspot_rms_comparison_low_goal_resolution.table
HifiMappingModeDBSRaster
HifiMappingModeFastDBSCross
HifiMappingModeFastDBSRaster
HifiMappingModeFSwitchOTF
HifiMappingModeLoadChopOTF
HifiMappingModeOTF
HifiPointModeDBS
HifiPointModeFastDBS
HifiPointModeFSwitch
HifiPointModeLoadChop
HifiPointModePositionSwitch
HifiPointProcDBS
HifiSScanModeDBS
HifiSScanModeFastDBS
HifiSScanModeFSwitch
HifiSScanModeLoadChop
279-1342190765
279-1342190763
279-1342190762
278-1342190812
278-1342190811
278-1342190810
278-1342190809
278-1342190806
278-1342190805
277-1342190743
277-1342190738
277-1342190736
277-1342190735
277-1342190734
267-1342190219
267-1342190216
267-1342190214
267-1342190212
267-1342190208
267-1342190207
266-1342190200
266-1342190199
266-1342190198
266-1342190197
266-1342190196
266-1342190195
266-1342190193
266-1342190192
266-1342190191
266-1342190190
266-1342190187
266-1342190186
266-1342190185
266-1342190184
266-1342190183
266-1342190182
265-1342190160
265-1342190157
265-1342190156
264-1342190243
264-1342190242
264-1342190241
264-1342190240
264-1342190239
264-1342190238
264-1342190237
264-1342190234
264-1342190233
264-1342190232
264-1342190231
264-1342190230
264-1342190229
264-1342190227
263-1342190101
263-1342190099
263-1342190098
263-1342190097
263-1342190096
0
2
4
6
8
10

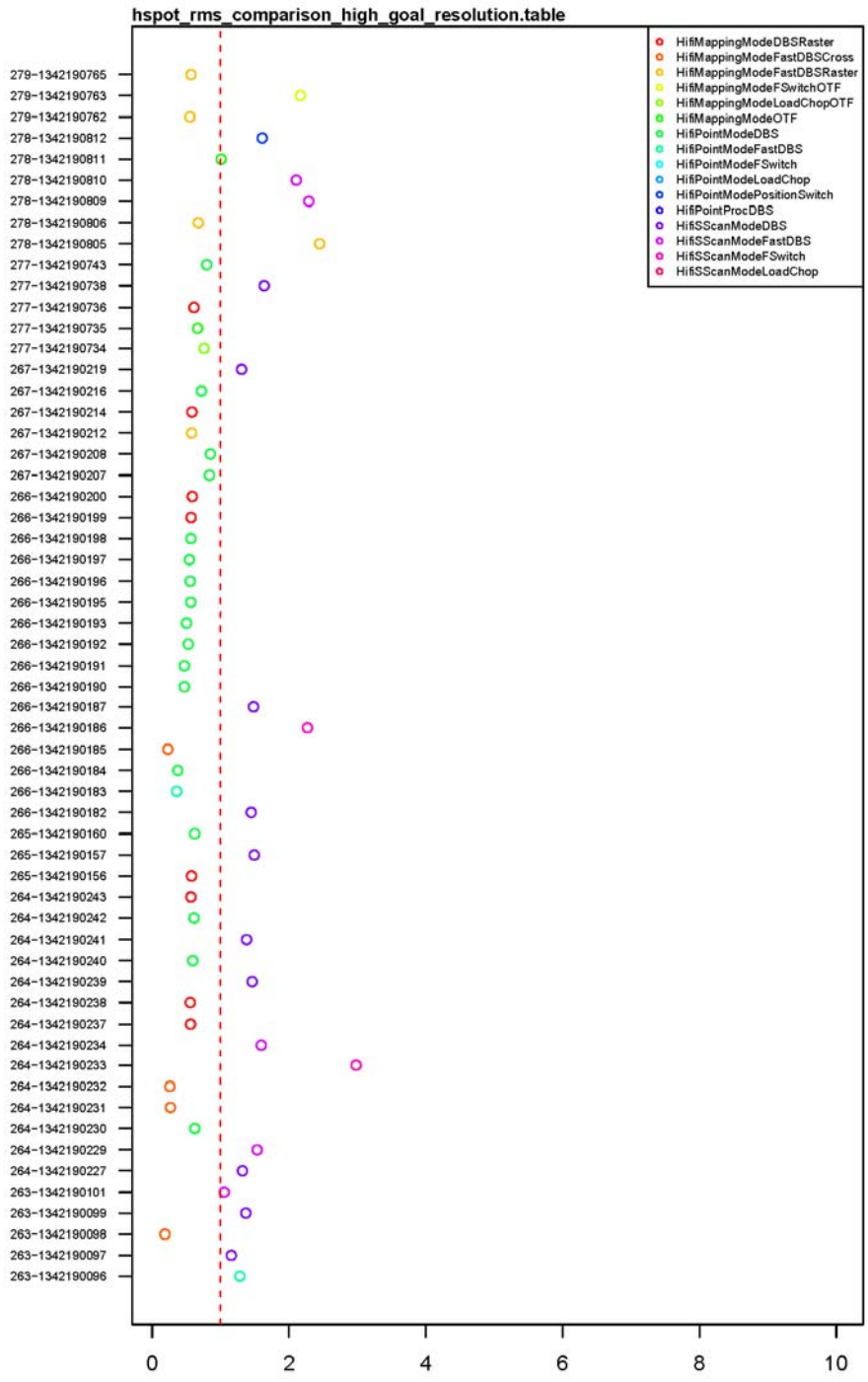

Figure 1: Ratios of measured to predicted (HSpot) noise for observations carried out in PV-II through February 25, with data smoothed to the goal low resolution (top) and high resolution (bottom). All testmode observations are included.

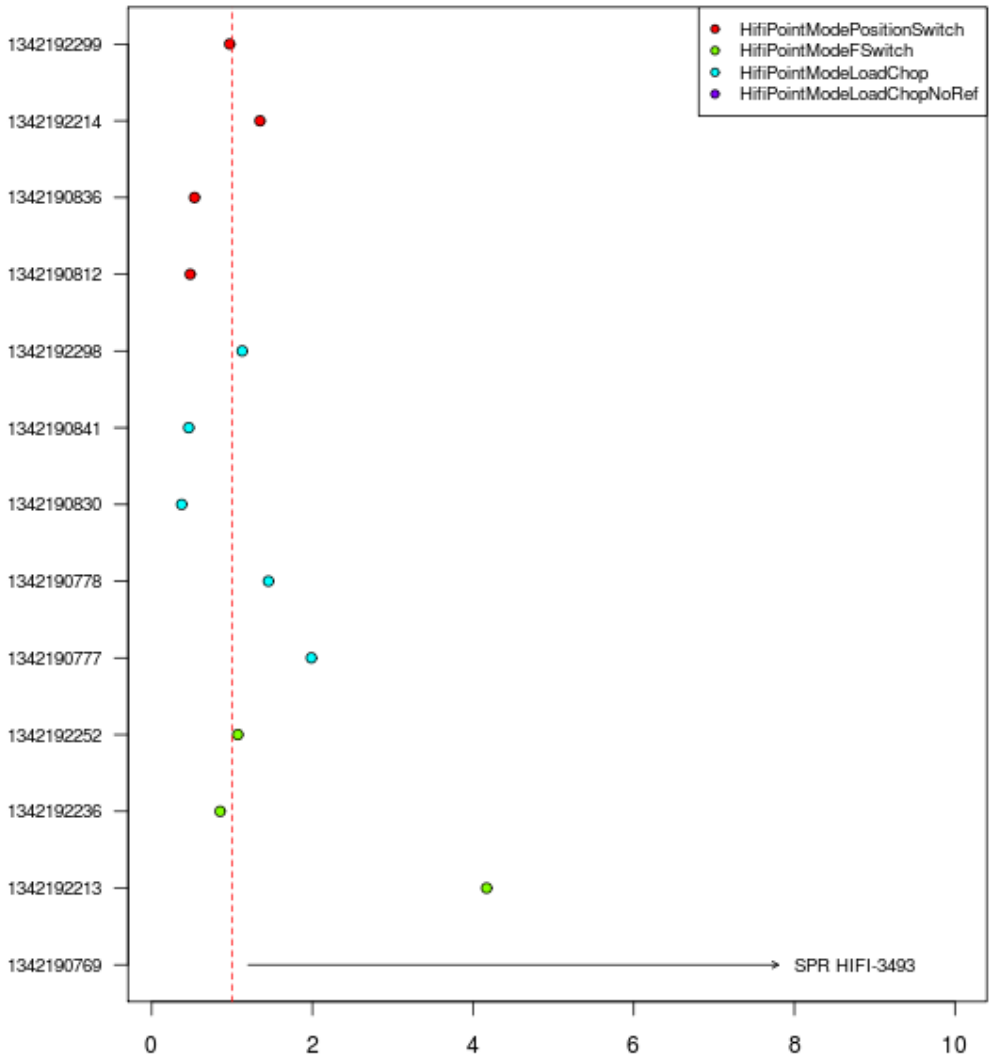

Figure 2: Ratios of measured to predicted (HSpot) noise for all non-DBS Point AOT observations carried out in PV-II through March 17, with data smoothed to the goal high resolution. The plot represents 13 of 16 scheduled observations, where three were not carried out successfully due to a Single Event Upset on OD305, and are to be recovered during Routine Phase calibration time. The largest outlier (1342190769) is a PointFSwitch observation in Band 7b with extremely poor baseline quality. The PointFSwitch mode is not released for science in the HEB bands.

The noise values for the Spectral Scans shown in Figure 1 have been measured from the dual sideband (un-deconvolved) H+V averaged spectra at the reference frequency where noise is predicted in HSpot, and have thus been appropriately scaled by a factor [2 x redundancy] $^{-1/2}$. Normally one would measure the noise at the reference frequency in the single-sideband, H+V averaged spectra (see Sec. 5.2). Numbers for the Spectral Scans are anyway given above to show the reasonably good agreement between predicted and measured noise before

deconvolution, which may itself influence data quality depending on pre-treatment of artefacts, baseline drifts, standing waves, etc.

In Figure 2 it is worth mentioning that the outlier PointFSwitch observation (1342192213) represents a limitation to measure the baseline RMS noise when the spectrum is rich and complex, making the definition of a mask for the measurements difficult; see Figure 3. Therefore this case does not represent a performance issue.

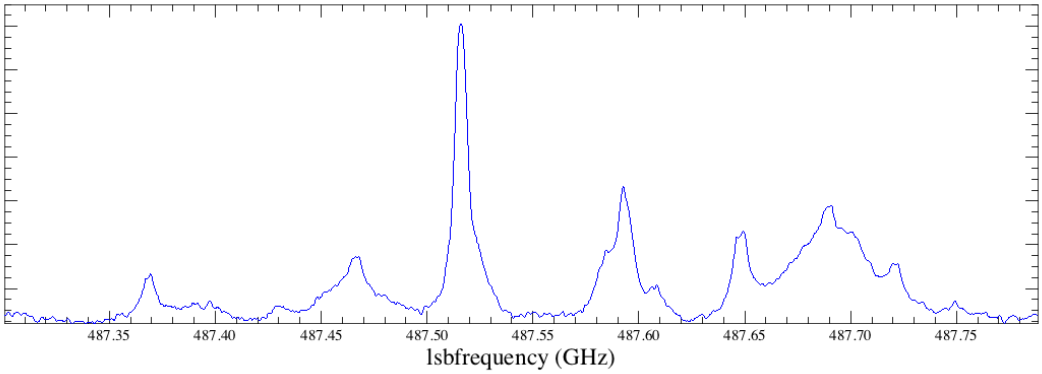

Figure 3: Obsid 1342192213, a PointFSwitch observation (unfolded) in Band 1a.

5.2 Spectral Scans (DBS and FastDBS)

The noise in the Spectral Scans when measured before sideband deconvolution scales with [2 x redundancy] $^{-1/2}$, to the SSB noise when the gains are equal (0.5). When the gains deviate from unity, the deconvolution algorithm should model these as well and the same scaling should apply. So far there are no indications of a departure away from unity that can be distinguished from many other data qualities.

While the analysis of the ~4 dozen Spectral Scans taken in PV-II so far is still ongoing, the deconvolved SSB RMS values are found to be in good agreement, but also sometimes 1.5 to 2 times higher than the HSpot predictions in Bands 1-5. A few examples are tabulated below for comparison to the points in Figure *1*. (note that the noise has not necessarily been measured at the reference frequency, but rather close to the middle of the covered range). Very preliminary results indicate that the HEB Bands 6 & 7 may yield even higher SSB RMS noise values - between 2-3 times than predicted by HSpot. Further tests with the software, and observations still to be carried out, are needed to confirm these findings.

1342190187 1b DBS R = 8, H+V HSpot T_{mb} noise @ 1 MHz = 22mK

Freq	H+V avg (T_{mb})
558.35	25.48
568.56	20.26
578.00	21.45
584.83	27.87

Ratio: 0.9-1.3

1342190239 2a DBS R = 8, H+V HSpot T_{mb} noise @ 3 MHz = 9 mK

Freq	H+V avg (T_{mb})
683.75	9.67

Ratio: 1.07

1342190241 2a DBS R = 3, H+V HSpot T_{mb} noise @ 3 MHz = 9 mK

Freq	H+V avg (T_{mb})
683.75	10.53

Ratio: 1.17

1342190215 5a DBS R = 8, H+V HSpot T_{mb} noise @ 3 MHz = 43 mK

Freq	H+V avg (T_{mb})
1163.90	78.08

Ratio: 1.81

1342190904 5a FastDBS R = 8, HSpot H+V T_{mb} noise @ 3 MHz = 46 mK

Freq	H+V avg (T_{mb})
1163.90	74.60

Ratio: 1.61

It is clear that effective sensitivity is enhanced after sideband deconvolution. Lines that are undetectable in individual double sideband spectra may become visible in deconvolved spectral as shown in Figure *4*.

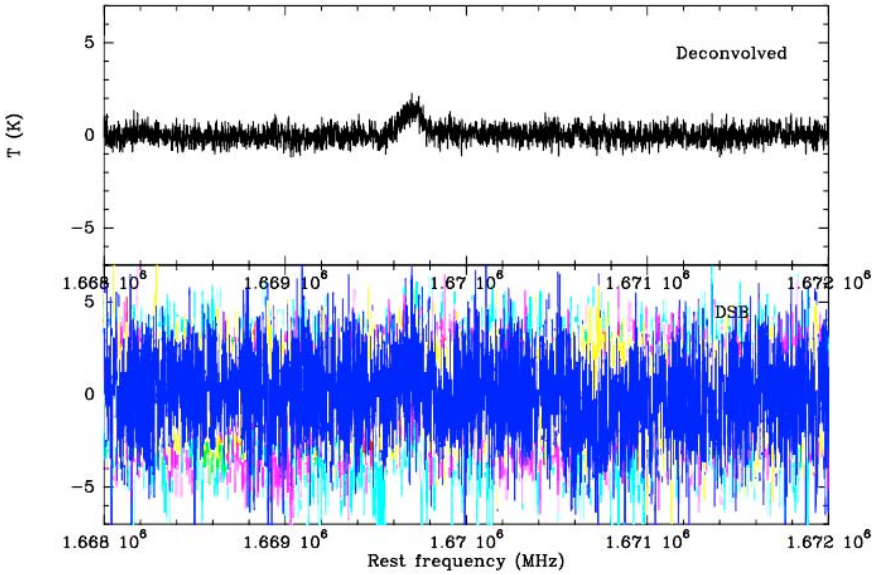

Figure 4: A survey of band 6b double sideband spectra taken at redundancy 8 with a fast-chop is overplotted in color in the lower panel, and the deconvolved single sideband spectra shown in top panel. The water line, invisible in the DSB dataset, is brought-out by the deconvolution.

There is not yet a clear distinction in noise performances between which use DBS and FastDBS observations (whereas it is reasonably clear that there is no distinction for fixed LO observations), but fast-chopping anyway will be more effective at removing standing waves in Bands 6 and 7.

Observers should keep in mind that the production of good SSB spectra is highly dependent on the removal all artefacts: standing waves, spurs, and the removal of all continuum baselines (linear or non-linear) prior to performing the deconvolution reduction step. An example of the value of “cleaning-up” spectra prior to deconvolution is shown in Figure 5.

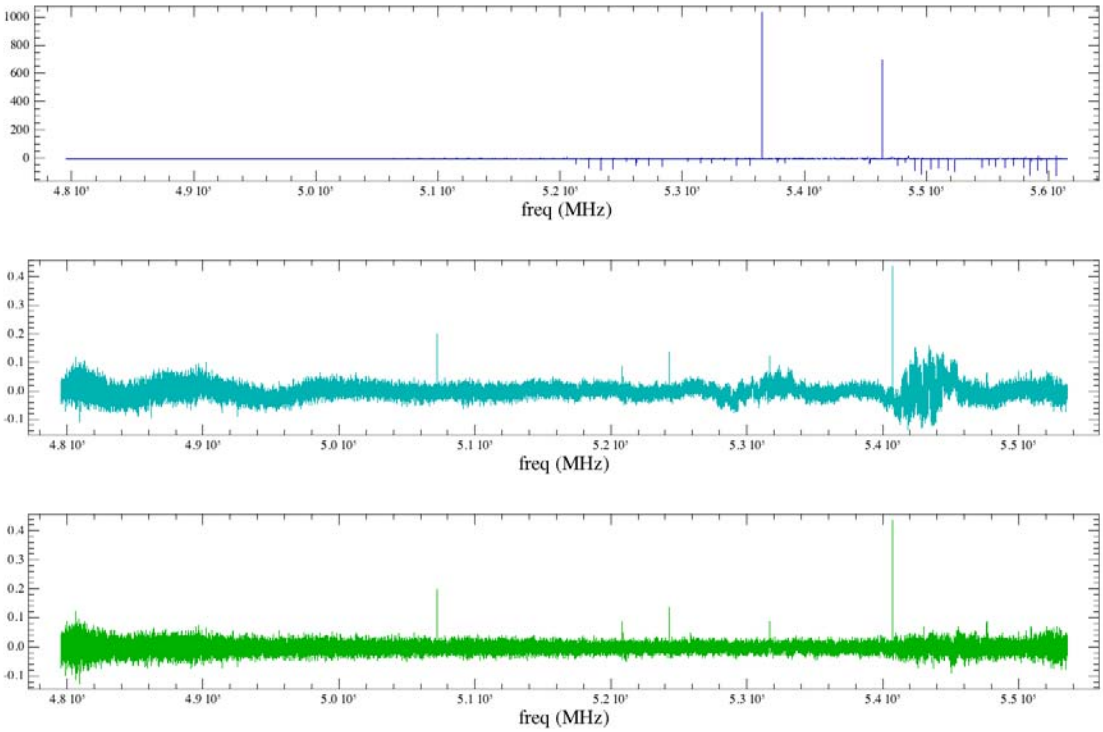

Figure 5: Band 1a spectral scan in various states of cleaning. The top plot shows the raw output from deconvolution. The effect of the spurs is obvious, as they echo throughout the solution. The centre plot has the spurs flagged-out, and the solution is much better, though issues with baselines are apparent. We applied a simple baseline removal routine, and the result is the spectrum on the bottom.

Summarizing the Spectral Scan observational results:

- The results have been generally very good, with nearly the expected noise levels in the spectral surveys regularly reached in most bands (within a factor of 1.5) with very comparable results obtained in both polarizations
- Both broad surveys (20-80 GHz in width) and narrow surveys (4-19 GHz in width) have been successfully observed and deconvolved. These include the so called “mini-surveys” which sample a narrow 4-6 GHz band without moving completely off of the target line while observing at high redundancy (R=12). These mini-surveys are useful in ruling out line blending and frequency ambiguities.
- No “ghost lines”, symptoms of instabilities or insufficient sampling, have been found in any survey. When spectral artefacts and bad baselines are removed completely from the input prior to deconvolution, the deconvolution yields flat baselines with neither ringing, nor any added repetitive noise structures.

5.3 Spectral Scans (FSwitch and LChop)

These modes are not yet released.

5.4 HIFI tuning ranges

In addition to certain known impure frequencies (see Sec. 4), the various HIFI LO chains have frequency ranges in which they cannot provide enough output power in order to sufficiently pump the mixers. The receiver noise temperature is very high in these ranges. Unlike the purity issues, however, there is little improvement to be expected on the short term so these areas must be considered as regions of low performance, over the spectral coverage currently achievable by HIFI.

While the border between sensitive and non-sensitive ranges is not abrupt and the noise degradation is often gradual, the band edges are defined and set in HSpot to avoid frequencies where the mixers are not even marginally pumped. Between the formal (HSpot) band limits, Users are able to recognize LO frequencies which offer lower performances from the output of time estimation in HSpot: at the requested LO frequency (Point and Map AOTs), the noise temperature is quoted in the Message window. The effect of higher noise temperature is to increase the observing time at a fixed noise goal (entered by the User), or conversely to reduce the S/N ratio at a fixed observing time goal. It is always worthwhile for the User to attempt to find a setting which minimizes the noise, where some flexibility is allowed in the IF placement of the spectral line(s) of interest. Note that system temperatures have been measured to a granularity of ~2 GHz, and therefore only significant differences may be noticed when changing the LO frequency that switches the target line(s) from one image band to the other.

The plots below illustrate the overall distribution of the receiver noise temperatures as measured in flight. All temperatures are the median DSB receiver temperatures over the full WBS bandwidth, in K. Frequencies are in GHz.

As can be seen from the plots, there are two types of poor sensitivity ranges:

- Those with a marginally, but still pumped mixer. They show up as receiver temperatures of the order of 2-3 times the average temperatures. Those frequency areas are considered in the range offered in HSpot, and will be scanned through during spectral scan, usually with an integration time doubled compared with other frequencies.

- Those where the mixer cannot be pump at all. Such ranges at band edges have been cut off from the HSpot front-end frequency ranges so that no time is spent observing at those frequencies. When those holes occur in the middle of a band, they are still offered to the User, and will be scanned through during spectral scan, usually with an integration time doubled compared with other frequencies. However, at those frequencies, the data may have to be discarded for an optimum SSB deconvolution. Only bands 4a, 4b and 6a are concerned by this situation. *It should also be noted that there can be*

sensitivity issues at the upper end of 7b (above 1898 GHz); despite of having enough LO power the tuning algorithm is not fully stable there. See the discussion of this in Sec. 4. Corrections to this are under investigation.

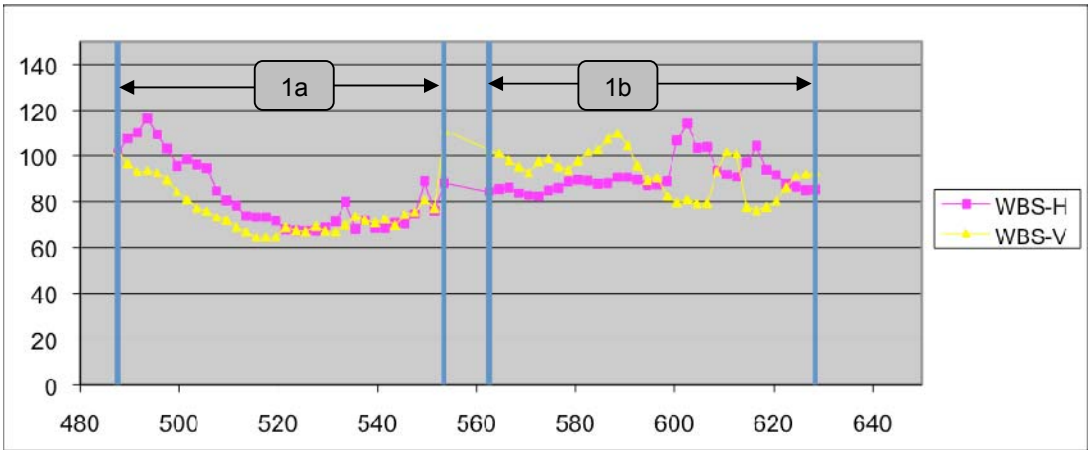

Figure 6: Band 1a/1b receiver temperature distribution

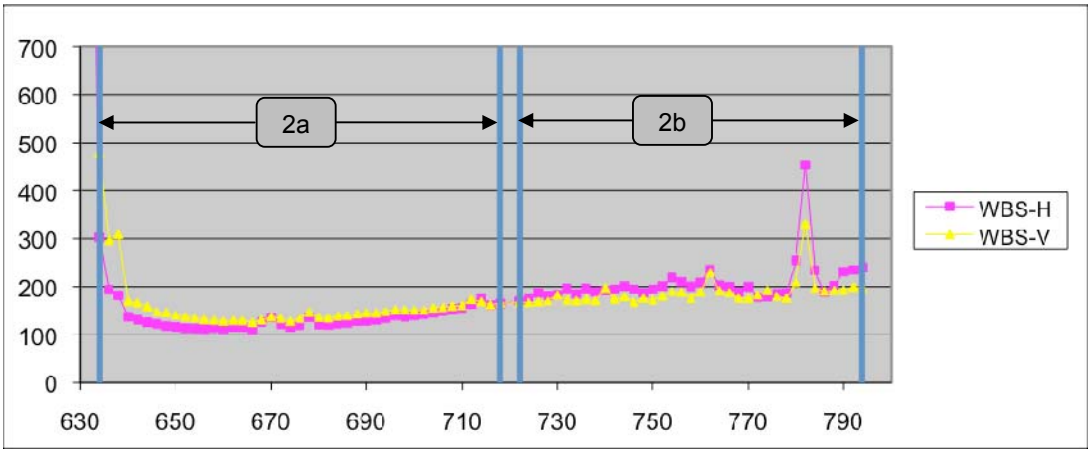

Figure 7: Band 2a/2b receiver temperature distribution

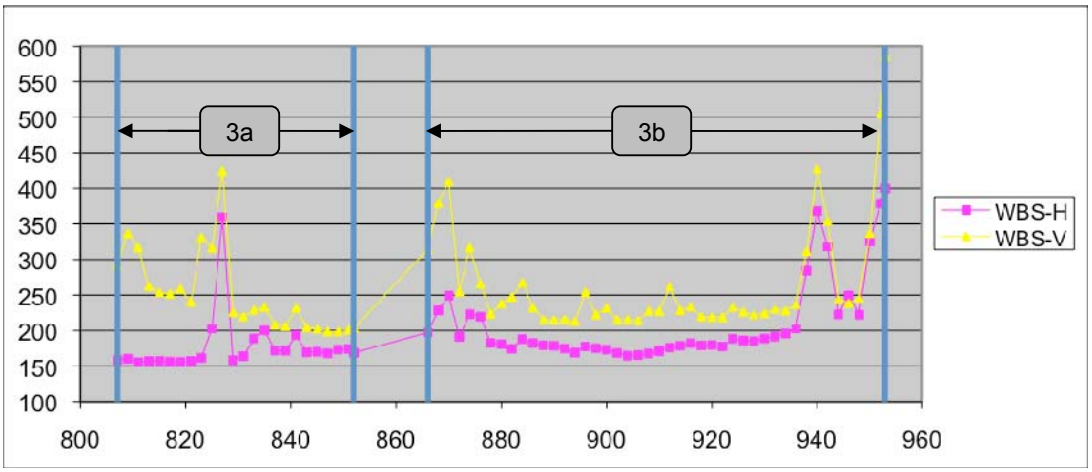

Figure 8: Band 3a/3b receiver temperature distribution

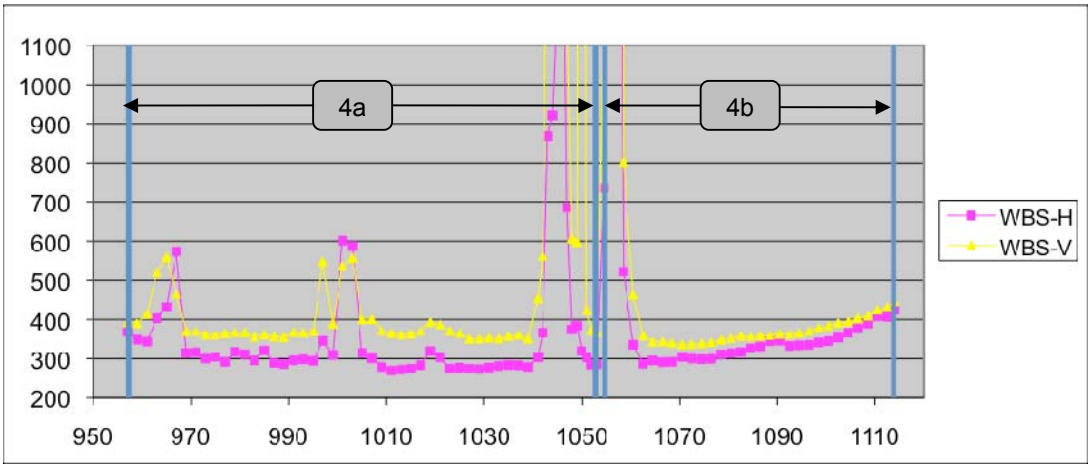

Figure 9: Band 4a/4b receiver temperature distribution

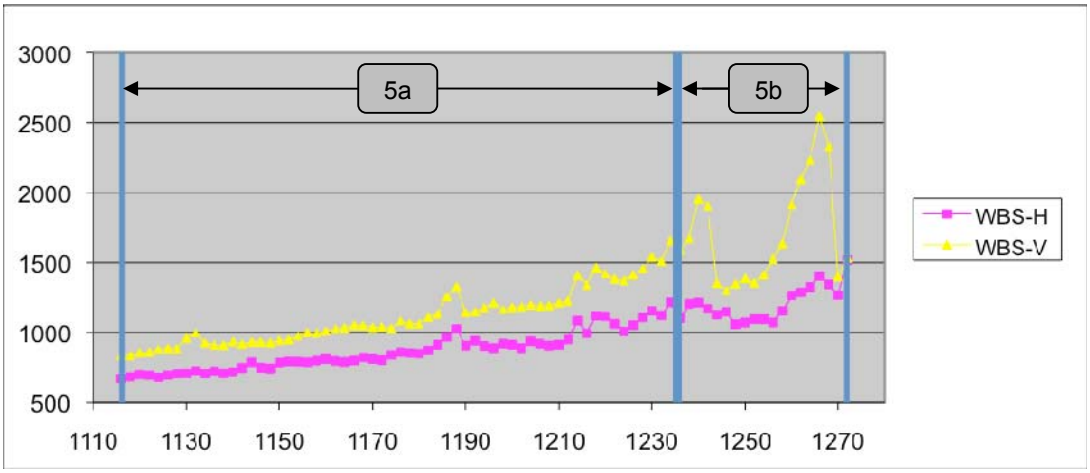

Figure 10: Band 5a/5b receiver temperature distribution

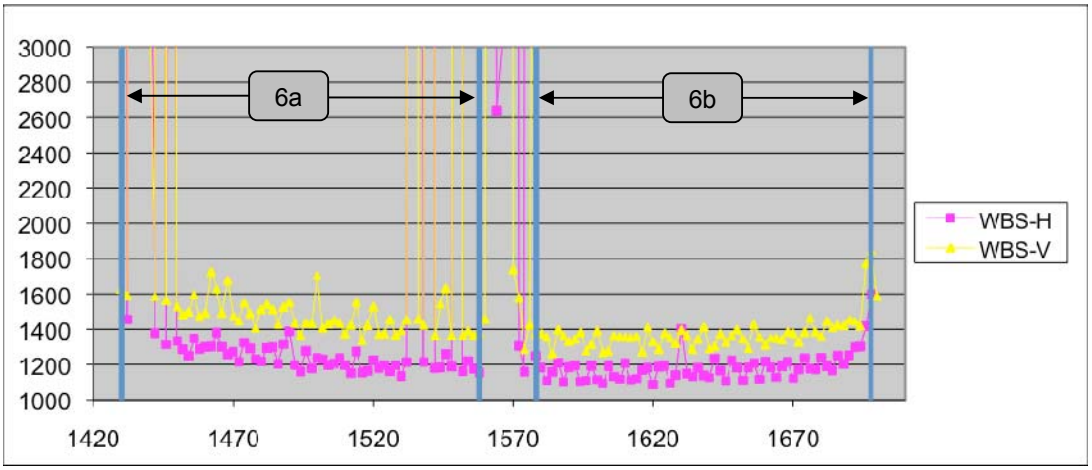

Figure 11: Band 6a/6b receiver temperature distribution

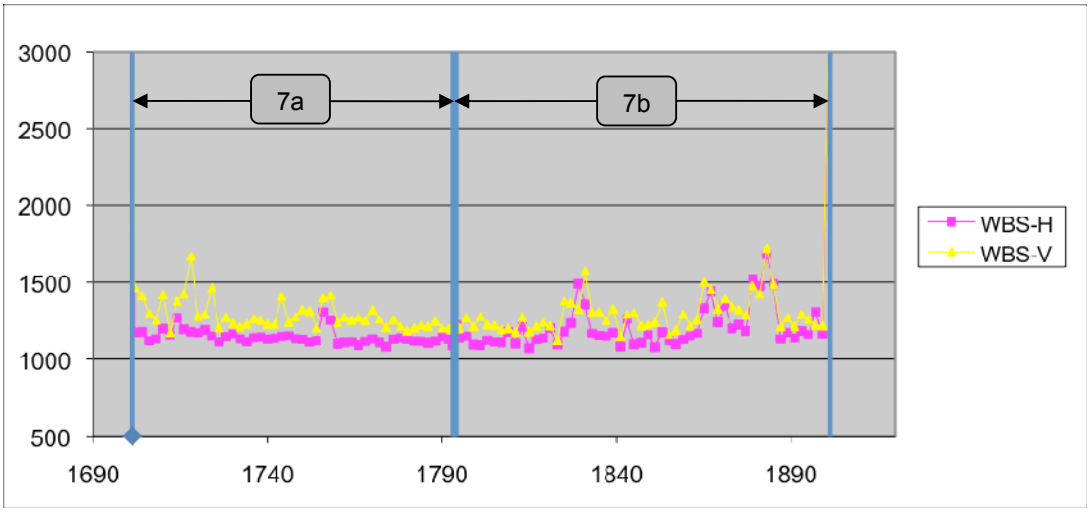

Figure 12: Band 7a/7b receiver temperature distribution

6. Performance/Sensitivities at IF Edges

In the diplexer bands 3, 4, 6 and 7, a substantial increase in system temperatures and thus decrease in sensitivity occurs towards the edges of the IF bandpass.

For Bands 3 and 4, the IF bandpass span is 4 GHz (4 – 8 GHz), and the last 500 MHz at either side, between 4.0-4.5 GHz and between 7.5-8.0 GHz, induces a significant increase of baseline noise since the diplexer mechanism introduces extra losses in those locations, and Tsys can increase up to 50-100% as compared to the central part of the IF (see Figure 13).

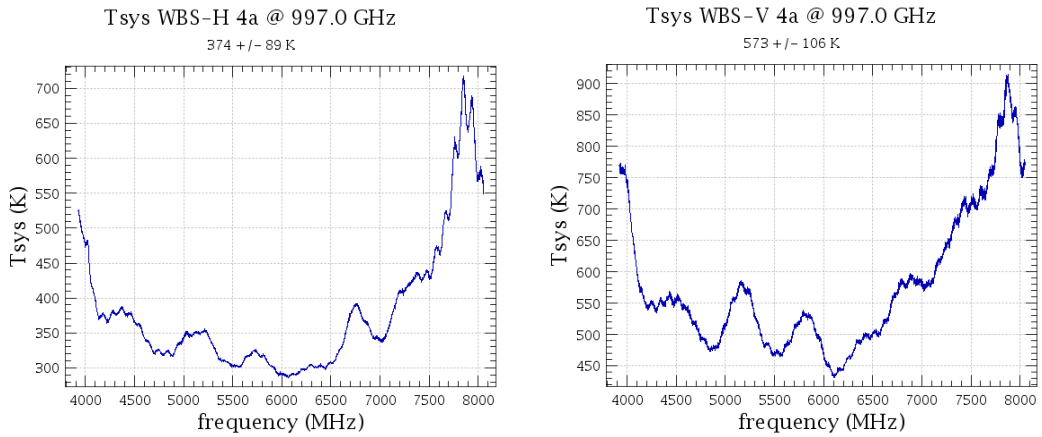

Figure 13: IF noise temperatures for the 4a LO chain tuned to 997.0 GHz.

Additional drawbacks include degraded stability performance (stronger standing waves and poorer baseline performance). Note that those stability issues can be mitigated by using Fast-DBS, but not the sensitivity degradation.

Thus it is not so much a lien or caveat on the Observing Modes, but rather a recommendation to avoid placing lines in the last ~500 MHz on either end of the IF in Bands 3 and 4, and in the last ~250 MHz in Bands 6 and 7, when using modes of the Point or Map AOTs. In cases where two lines are being targeted in the edges of the upper and lower sideband in a single AOR, it is better to devise separate AORs for each line despite the additional 180 sec slew tax, since time is not being saved in a single AOR when the noise and standing waves are impeding spectrum quality. Figure 14 shows an example of the kind of setup which is not recommended.

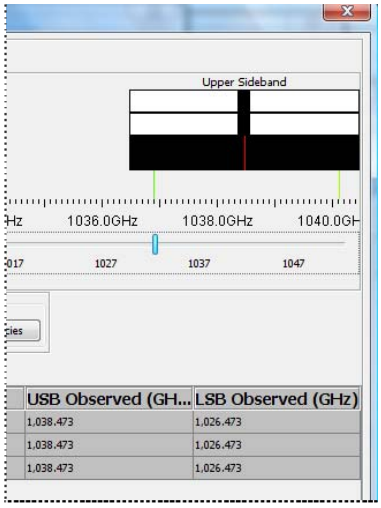

Figure 14: Example of a setup to avoid in Point or Map AORs, targeting lines at the edges of the IF in either or both of the USB or LSB in diplexer bands. Two separate AORs should be devised.

7. Standing Wave Residuals after Calibration (Level 2)

The HIFI pipelines are designed to correct for standing waves in the astronomical data using off-source sky spectra taken in AORs using any of the observing modes that include OFF-source sky measurements, i.e., telescope nodding plus chopping with the internal M3 mirror with fixed throws on the sky (the DBS modes), or else telescope nodding to a User-selected reference sky position (modes using a position switch). A summary is given of the presence of *residual* standing waves in Level 2 data taken with the Point AOTs that have all been reference-corrected in the standard fashion. FSwitch and LChop observations have all included the sky reference option in HSpot. [Approximations can be made in IA for skipping this option to a corresponding "No Ref" version as allowed in HSpot, by simply skipping the sky correction step in the pipeline.]

Attempts to remove these waves in HIPE are also discussed. Because the wave characteristics differ between bands with beam splitters and diplexers as well as between SiS and HEB mixers, they are discussed separately. It is acknowledged that PV does not allow for a complete matrix of observations in every band with every mode and full set of relevant options, so conclusions are preliminary and weighted towards the bands and modes most requested in the PSP/SDP AORs..

7.1 Bands 1-5 (SiS mixers)

7.1.1 DBS modes

Bands 1-5 data taken in DBS mode generally do not show standing waves at Level 2. Exceptions are sometimes observed, however, and in these cases the User can remove the waves with the sine wave fitting task 'FitHifiFringe' in HIPE.

Two cases are shown below.

- In Band 4b the diplexer causes a 650 MHz ripple. Figure 15 shows a sine wave fit (red) relative to a baseline (green), automatically determined with FitHifiFringe.

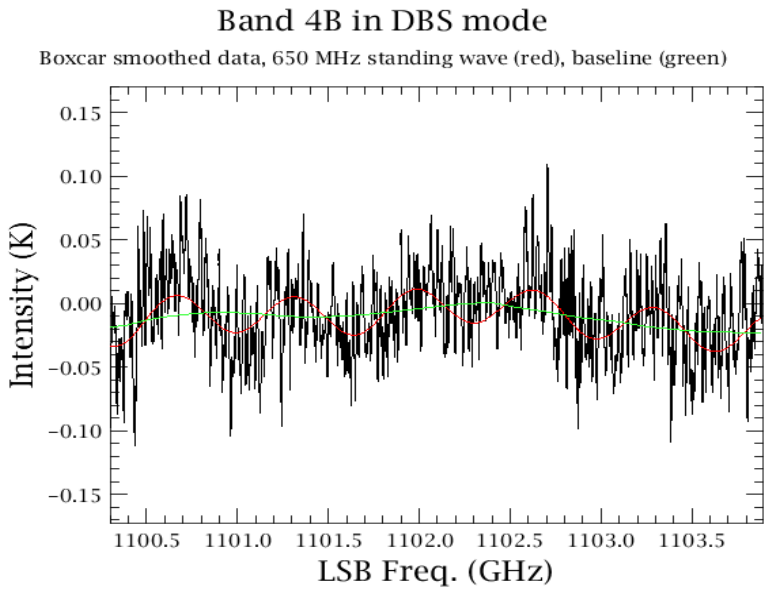

Figure 15: Standing wave residual at Level 2 in a DBS observation, with the fitted sine wave (red) relative to a smoothed baseline (green).

- Strong continuum sources show the effect of ripples in the passband calibration. The periods are typically in the 90-100 MHz range, and the amplitudes are at most 2% relative to the continuum. See Figure 16 below for a case where 92 and 98 MHz since waves are present.

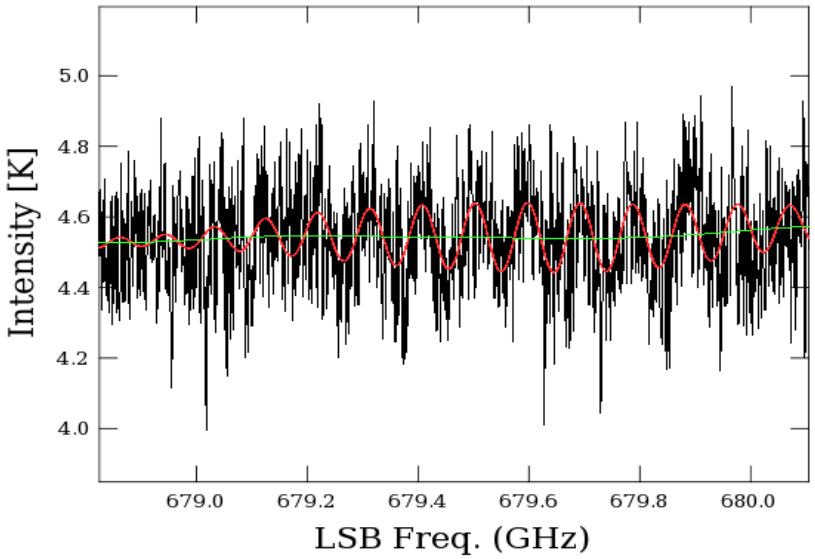

Figure 16: Strong continuum source with two standing wave components (red), relative to the baseline (green).

7.1.2 PosSwitch, FSwitch, LChop modes

Calibrated observations taken with the simple PosSwitch, FSwitch (with PosSwitch), or LChop (with PosSwitch) modes in beamsplitter Bands 1, 2, and 5 also show the cleanest spectra. If any residual waves are present in the Level 2 products, they have the shape of pure sine waves and can be subtracted using the FitHifiFringe task in HIPE.

Observations in diplexer Bands 3 and 4 often show residual waves with larger amplitudes compared to the DBS modes. Waves generated in the diplexer rooftop are not pure sine waves. Amplitudes increase strongly toward the IF band edges. It is thus always advised to place the line of interest near the middle of the IF band when possible, in WBS sub-bands 2 or 3. Although FitHifiFringe only fits sine waves, fits to the diplexer waves can be approximated using multiple sine waves, typically around 600 MHz. The approximation is not as good at the IF band edges. Examples are shown for Bands 3 and 4 below. Note that the baseline is strongly curved in both observations, and the user will need to remove those separately in HIPE, using polynomials.

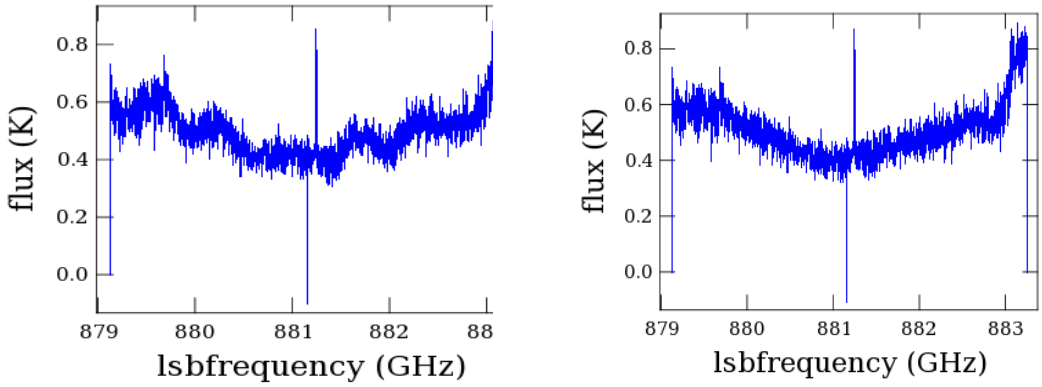

Figure 17: Band 3b observation using PointFSwitch at Level 2 after sky subtraction (left) and after interactive fringe fitting and removal (right). Note the poor edges in the spectrum on the right.

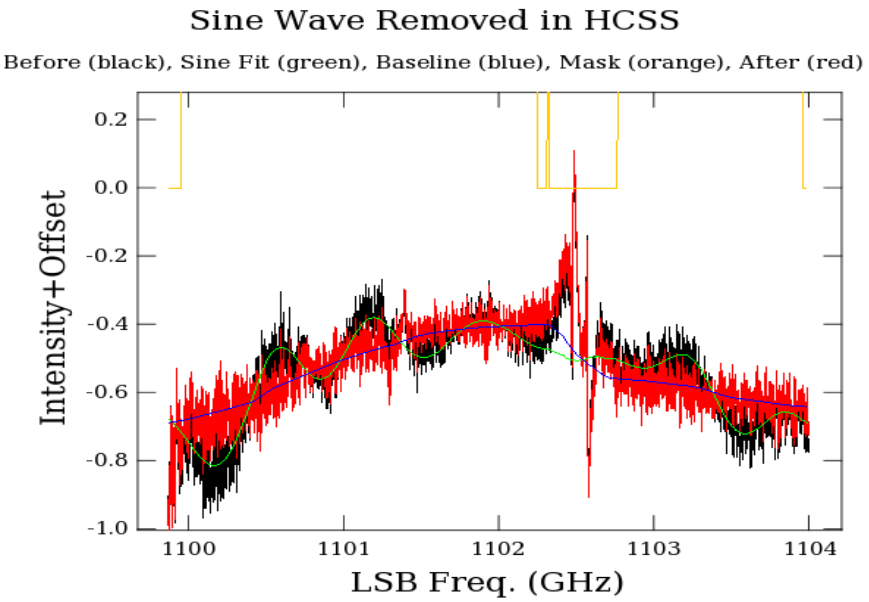

Figure 18: Band 4b observation using PointFSwitch, showing a strong residual standing wave (black). Its period (~600 MHz) and increasing amplitude toward the band edges are those expected for diplexer bands. It was fitted with a combination of sine waves using FitHifiFringe (green). The corrected spectrum (red) still shows a strongly curved baseline that can be subtracted with a polynomial fit in HIPE.

7.2 Bands 6-7 (HEB mixers)

The HEB mixers generate waves with characteristics that depend on the mixer current level, but since there is a dependence on LO power which may not be stabilized (between ON and OFF spectra), both electronic and optical standing wave residuals can be mixed together. Data taken with all observing modes analyzed so far show residuals at Level 2, where the non-DBS modes tend to show larger and more complex residuals.

7.2.1 DBS Modes

Bands 6-7 are less stable than bands 1-5, and Level 2 data occasionally show residual waves. Examples are shown in Figure 19 for portions of Bands 6a and 7b. The latter was box-car smoothed by 5 channels.

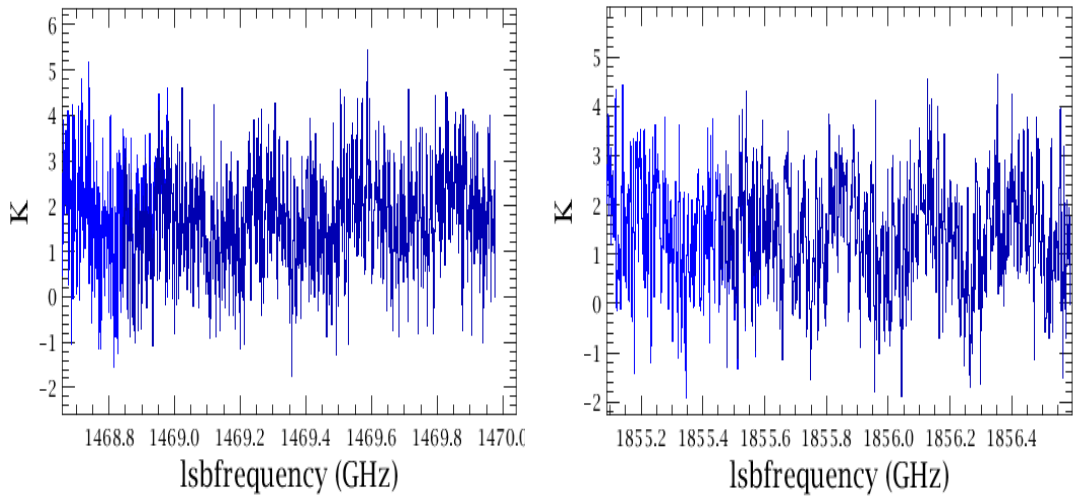

Figure 19: Standing wave residuals in Band 6a (left) and 7b (right).

These 'electronic' standing waves have periods of ~300 MHz, but they are not sine waves and 'FitHifiFringe' can only approximately remove them. A promising method ('current matching technique') is being developed to remove these waves in the pipeline.

As for the presence of these waves the following general guidelines can be given:

- Band 6b is most stable and is least affected.
- FastDBS mode spectra tend to show weaker standing waves than 'slow chop' DBS mode spectra
- In Band 7, spectra taken with the vertical polarization spectrometers tend to show stronger waves than from the horizontal polarization. Sometimes this effect is very strong, as shown in the Band 7a observations below (Figures Figure *20* and Figure *21*).

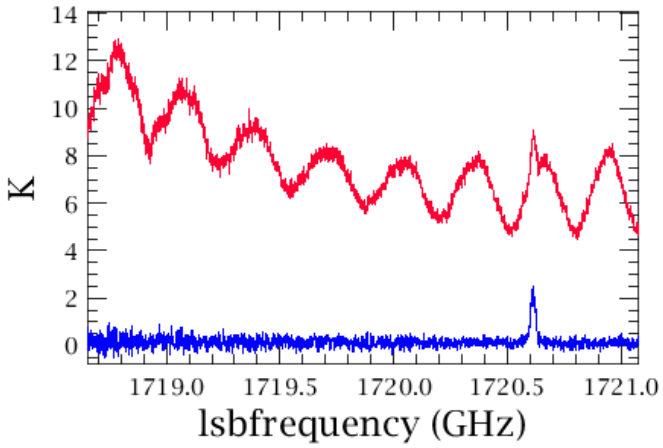

Figure 20: Standing wave pattern in the Level 2 in Band 7a for WBS-V (red) and WBS-H (blue).

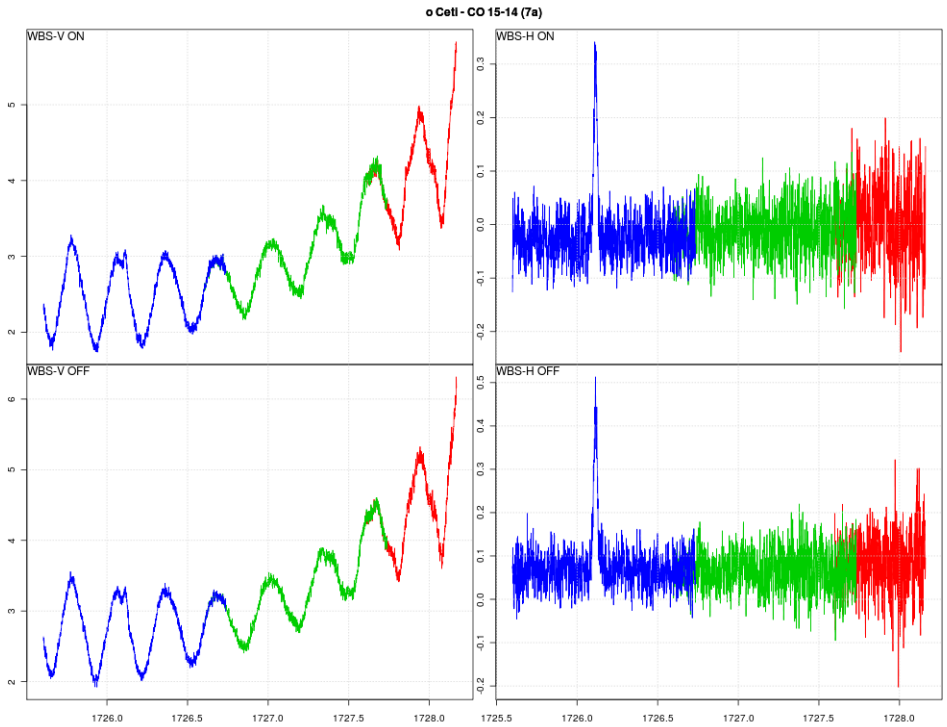

Figure 21: During the analysis of the FPG-3 raster map done on OD 278 (obsid 1342190805:Fpg3_M_FastDBSNoC_7a_CO_15-14_oCeti_3x3) it was found that the quality of the WBS-V has much poorer data quality, due to a large ripple, than WBS-H. The latter shows hardly any ripple at all. These data were processed using the "level1WithoutOffSubtr" algorithm and the attached plot shows both the ON and OFF phase for both polarizations. As can be seen the ripple in V in the ON and OFF phase will not cancel when averaged. When subtracted, most of the ripple is gone, but so is the line.

7.2.2 PosSwitch, FSwitch, LChop modes

Non-DBS observations show rather strong residuals in Level 2 spectra. An effort is under way to provide alternative processing of HEB band observations such that appropriate OFF spectra are selected from a database of observations based on mixer current level (the 'current-matching' technique). This approach should reduce the amplitudes of the residual standing waves considerably, but is currently in development. Presently, the user may apply FitHifiFringe to remove the waves in Level 2 spectra. This method has limitations, because the HEB waves are not pure sine waves: they disperse over the IF band (i.e. their 'phase' changes). Examples are shown below for PointLChop and PointPSwitch observations. As can be seen, the line shape in the WBS-V and WBS-H spectra differ somewhat after subtracting the sine-wave fit. This highlights another limitation of FitHifiFringe: *for broad lines covering much of the IF, insufficient surrounding baseline may be left to obtain accurate sine wave fits. In addition, as for the diplexer bands, solutions are less accurate for lines close to the IF band edge.* Finally, we note that P_FSwitch observations in band 6 and 7 are still under investigation, and are currently not released because of strong standing waves and baseline drifts.

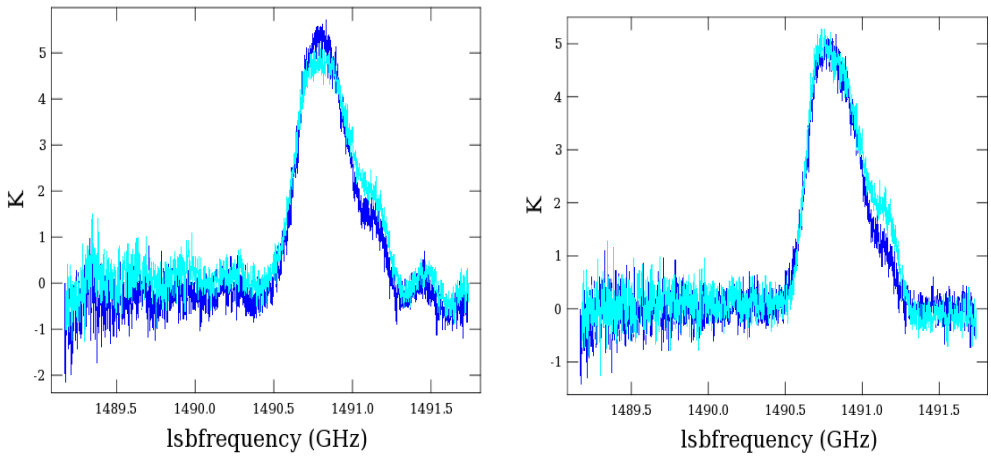

Figure 22: Band 6a PointLChop observation showing residual waves after standard level 2 pipeline processing (left), and after standing wave removal using FitHifiFringe (right). The fringe-corrected spectrum has been shifted and a small scaling applied along the intensity axis so that the H and V peaks agree.

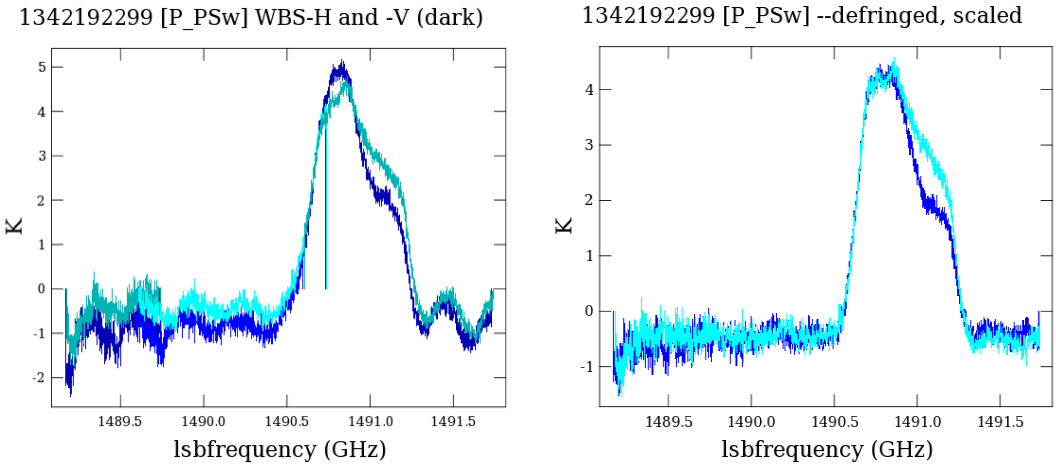

Figure 23: Same as Figure 22, using PointPSwitch.

8. Pointing

8.1 Focal Plane Geometry Calibrations "Part 3"

In PV-II a first set of FPG-3 observations were carried out, using CO and H_2O emission lines from AGB stars to check the pointing in a number of HIFI bands. They serve the following purposes:

- Check the performance of the (Fast) DBS raster and DBS cross mode.
- Establish the S/N of the observed spectral lines and their usefulness for pointing verifications.
- Build up a database of pointing results on which eventually a SIAM update for the HIFI aperture entries may be based.
- Provide a set of raster maps to cross-compare with OTF mapping modes.

8.2 Observations

OD	ObsId	Source	Size	Line	Band	Mode	Comment
264	1342190237	o Ceti	5 x 5	CO 6-5	2a	DBS	
264	1342190238	o Ceti	3 x 3	CO 6-5	2a	DBS	
264	1342190243	o Ceti	3 x 3	CO 6-5	2a	DBS	
265	1342190156	NML Tau	3 x 3	CO 11-10	5b	DBS	no detection
265	1342190161	o Ceti	3 x 3	CO 9-8	4a	DBS	
266	1342190179	o Ceti	3 x 3	CO 5-4	1b	DBS	Failed due to SEU
266	1342190199	o Ceti	3 x 3	CO 6-5	2a	DBS	
266	1342190200	NML Tau	3 x 3	CO 6-5	2a	DBS	
267	1342190212	o Ceti	3 x 3	CO 7-6	3a	FastDBS	
267	1342190214	o Ceti	3 x 3	CO 10-9	5a	DBS	
278	1342190805	o Ceti	3 x 3	CO 15-14	7a	FastBS	

278	1342190806	NML Tau	3 x 3	H_2O 303-212	7a	FastDBS
279	1342190762	o Ceti	3 x 3	CO 14-13	6b	FastDBS
279	1342190765	NML Tau	3 x 3	H_2O 212-101	6b	FastDBS
281	1342190844	o Ceti	3 x 3	CO 5-4	1b	DBS
283	1342190902	R Dor	cross	CO 10-9	5a	FastDBSX
283	1342190903	R Dor	cross	CO 10-9	5a	FastDBSX
283	1342190908	R Dor	3 x 3	CO 7-6	3a	FastDBS

Table 1: List of FPG-3 observations carried out in PV-II, Blocks 1 and 2.

Frequency	**El**	**transition**	**band**
MHz	*cm-1*		
576267.931	38.4481	5-4	1b
691473.076	57.6704	6-5	2a
806651.806	80.7354	7-6	3a
1036912.393	138.3904	9-8	4a
1151985.452	172.9780	10-9	5a
1267014.486	211.4041	11-10	5b
1611793.518	349.6975	14-13	6b
1726602.507	403.4612	15-14	7a

Table 2: CO transitions targeted as part of FPG-3.

8.3 Results

In the following we show individual spectra and integrated intensity maps for all ObsIds. Note, that the data were pipelined using a Level 1 *without OFF subtraction* algorithm, this in order to assess the pointing of the ON and OFF phase of the DBS raster scheme separately.

The individual spectra show baseline ripples with opposite phase as expected, the final DBS spectra (not shown here) therefore will have flat baselines. Because the spectral lines sit on top of the ripple at different phase, they do not match up perfectly in the spectrum maps.

Noteworthy is the non-detection of the CO 11-10 line and very weak detection of CO 6-5 in NML Tau. This latter observation was carried out immediately after the same line in o Ceti, which looks fine, so it is not expected that this observation suffers in any way from the aftermath of the SEU. In fact, the lines in NML Tau are expected to be considerably weaker and broader than in o Ceti, according to APEX results. The purity issues in Band 5b (Sec. 4) may complicate the detection as well. Note however, that NML Tau could be used to check pointing alignment in Band 7a, where the H_2O 3_{03} - 2_{12} 1721.3 GHz emission line is well detected in the same map (i.e. set up in the AOR to observe both possible lines).

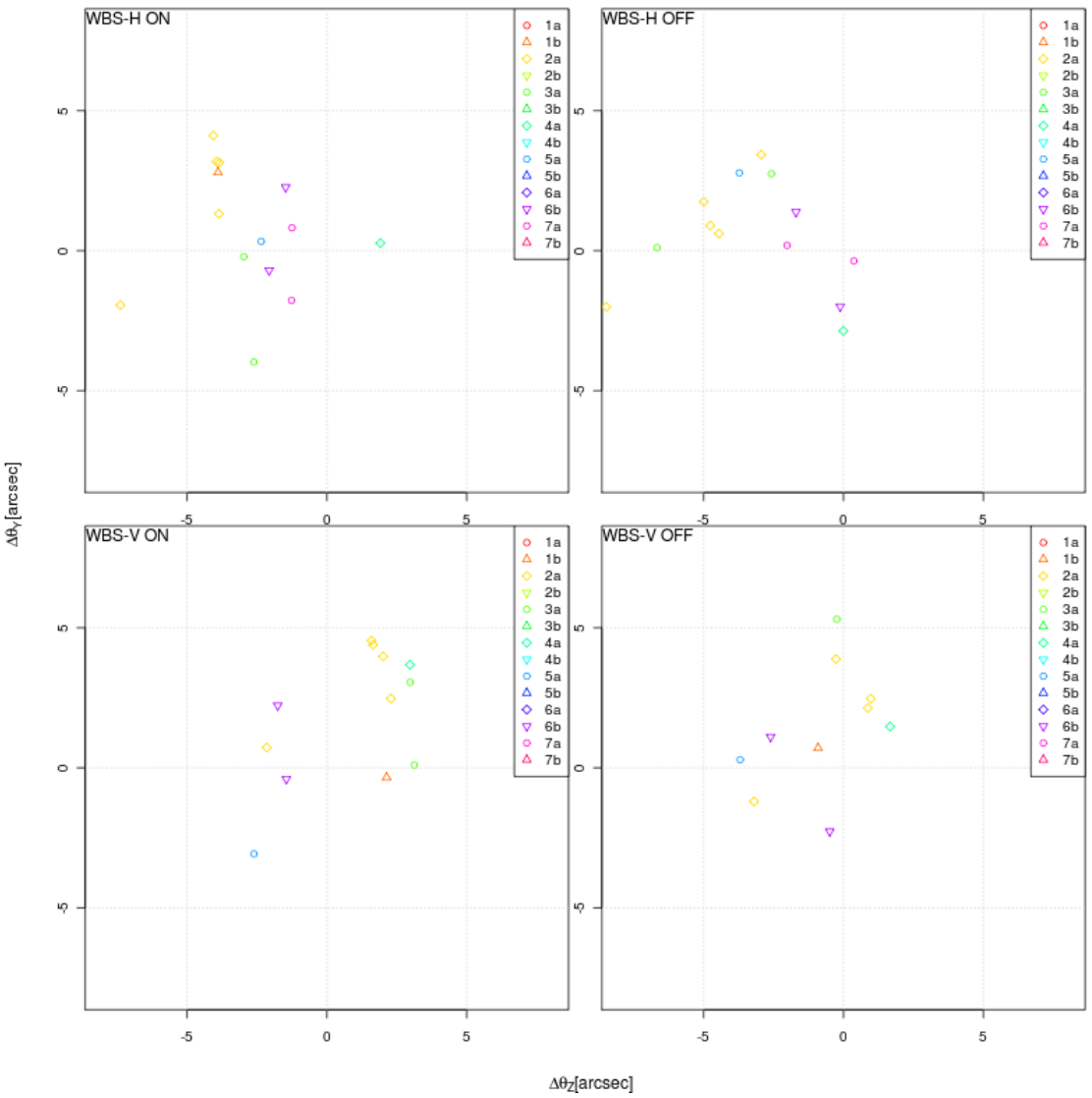

Figure 24: Observed and fitted focal plane offsets.

Figure *24* shows the fitted focal plane offsets colour coded by band. Note, that the measurements were all carried out using the SIAM entry for the synthesized HIFI beam in each band, which is an average of the beam positions of the H and V mixers (discussed further below in this section).

In all pointing maps observed during PV-II, the central grid position always showed the strongest signal, i.e. all of these observations would have succeeded as single point observations. Based on these results there is at present no need to update the HIFI SIAM entries.

The SIAM provides entries for the angular rotations from the telescope boresight (optical Attitude Control Axis) to the set of HIFI beams in the focal plane. The SIAM contains offsets for each of the seven H polarization mixer beams, one per band, and

corresponding so-called synthetic beams which are effectively the average of the H and V mixer beams in focal plane coordinates. The commanded pointing is always referenced to a synthetic beam as the prime instrument frame. Figure 25 schematically illustrates the offsets of the HIFI beams in the focal plane. These offsets should be kept in mind when comparing spectra from the two separate polarizations (taken simultaneously at slightly separated positions on the sky, and processed separately in the pipeline), especially on extended sources which may be intrinsically polarized at frequencies of interest.

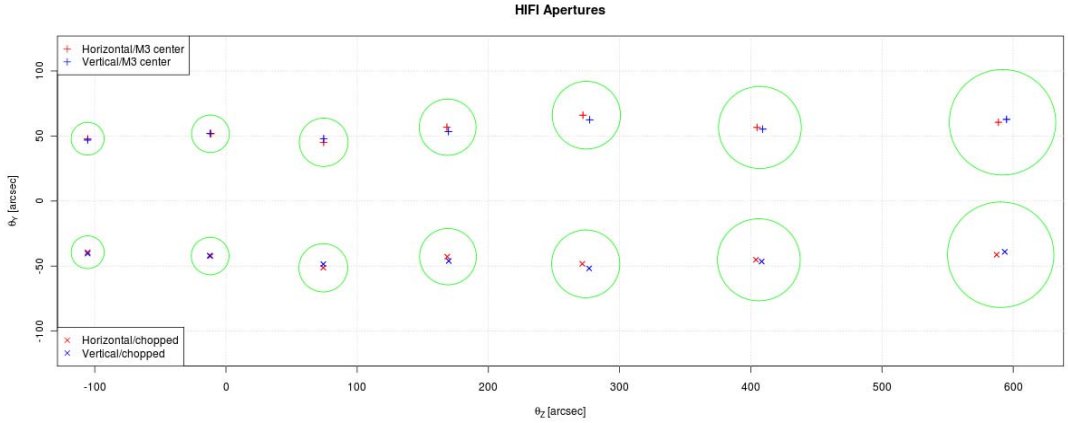

Figure 25: Locations of the HIFI apertures, highlighting the difference between H and V. Only H apertures are represented directly in the SIAM, the V entries are calculated from these and the locations of the synthesized beams, assuming a symmetric location of H and V with respect to the synthesized ones. The green circles represent HIFI FWHM beams centered on the synthesized beam locations.

Since the angular separation between the H and V beams may be important when interpreting observations on extended sources, the User may deduce the relative offsets directly from the SIAM with a script which is provided in the Appendix.

9. Intensity Calibrations

The 12 m APEX telescope uses a number of AGB stars as standard sources for line calibration. In particular the results obtained by Risacher and van der Tak [1] for the CO 6-5 line at 691.4730763 GHz offer the opportunity to compare with HIFI results during PV-II.

9.1 Observations

Table 3 lists operational day and ObsId for those observations which were analysed for this report.

OD	ObsId	Source	Observation
264	1342190237	o Ceti	DBSRaster
264	1342190238	o Ceti	DBSRaster

264	1342190243	o Ceti	DBSRaster
266	1342190199	o Ceti	DBSRaster
264	1342190242	R Dor	DBSPoint
264	1342190240	IK Tau	DBSPoint
266	1342190200	IK Tau	DBSRaster
266	1342190196	W Hya	DBSPoint

Table 3: List of observations

9.2 Results

Table Table *4* lists observed peak intensities and line widths, obtained by fitting Gaussian profiles to the observed lines. Note, that the assumption of this type of profile is not necessarily justified, e.g. o Ceti shows signs of self-absorbed CO lines. However, it allows a standard procedure to be used for the derivation of quantitative values for the purpose of this report.

		HIFI					APEX	
		H		V				
Obsid	**Source**	**peak**	**width**	**peak**	**width**	**H/V**	**peak**	**width**
		[K]	*[km/s]*	*[K]*	*[km/s]*		*[K]*	*[km/s]*
1342190237	o Ceti	3.29	5.4	3.51	5.4	0.94	34.5	4.8
1342190238	o Ceti	3.28	5.4	3.51	5.4	0.93		
1342190243	o Ceti	3.23	5.6	3.51	5.6	0.92		
1342190199	o Ceti	3.32	5.5	3.52	5.5	0.94		
1342190242	R Dor	1.52	9.1	1.66	9.1	0.92	17.1	9.1
1342190240	IK Tau	0.36	24.8	0.49	24.8	0.73	6.6	24.2
1342190200	IK Tau	0.39	25.9	0.49	25.9	0.80		
1342190196	W Hya	0.88	11.4	0.91	11.4	0.97	?	?

Table 4: Observed line intensities and widths.

The beam width of the Herschel telescope at the frequency of the CO 6-5 transition is Θ_H = 32.7”, whereas the APEX telescope has a HPBW of Θ_A = 9.5” at this frequency.

Given a source size Θ_S, also in arcsecs, the expected intensity scaling between main beam brightness temperatures observed by APEX (I_A) and HIFI (I_H) can be expressed as

$$I_H = I_A * (\Theta_S^2 + \Theta_A^2)/(\Theta_S^2 + \Theta_H^2)$$

Solving for the source size we get

$$\Theta_S^2 = (\Theta_A^2 I_A - \Theta_H^2 I_H)/(I_H - I_A) \qquad \text{(Eq. 1)}$$

Figure 26 shows the expected intensity ratio as a function of source size.

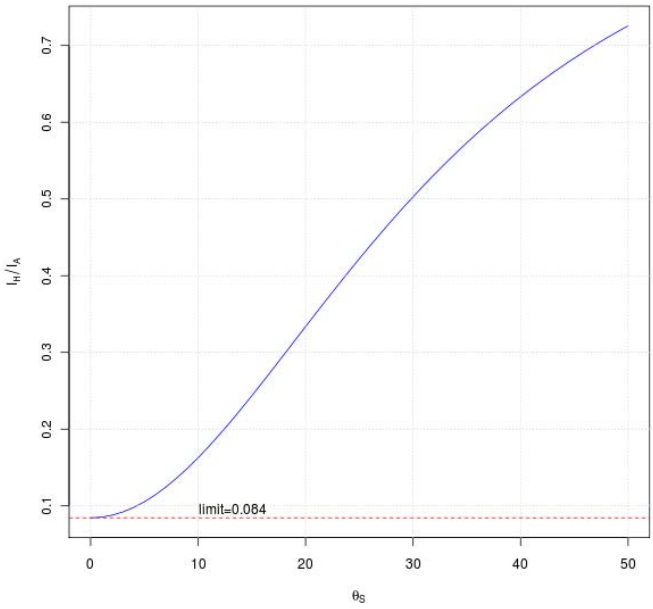

Figure 26: Expected ratio of HIFI to APEX main beam brightness as function of source size.

We use a main beam efficiency of η_{mb} = 0.74 to convert observed antenna temperatures for HIFI to a main beam brightness scale.

For o Ceti we get a source size of 4.1", corresponding to$7.8*10^{15}$ cm at an assumed distance of 128 pc. For R Dor the size calculated according to Eq. 1 is 3.2", or $2.9*10^{15}$ cm at a distance of 61 pc. Finally, for IK Tau Eq. 1 does not produce a real-valued solution for Θ_S, because the ratio I_H/I_A is lower than the value of 0.084 predicted by Eq. 1 in the limit of vanishing source size (see Fig. 3.1). Note, that there is also a very deviating H/V ratio for this source in Table 3.2. However, comparison with the predicted spectrum in section 1.7 (last panel of Fig. 3.4) shows no obvious problem with the observed intensities.

10. Frequencies and Velocities

Summarizing, no serious problems have been found with the frequency and velocity calibration in the HIFI pipeline. There are some issues which the User should be aware of when interpreting the frequency scales on Level 2 spectra. Until these issues are understood and fixed they will cause an error in the frequency scale of up to 2 km/s.

10.1 Outstanding Issues

- HCSS uses 19.5 km/s instead of 20.0 for lsr vel => < 0.5 km/s error, compared to the LSR frame used by the MPS. Additionally, the Sun is used instead of the SSBC => < 0.020 km/s error
- To compute the spacecraft velocity, HCSS uses an imprecise velocity of the earth with respect to the sun (and not the SSBC). This gives an error of ~< 1.5 km/s
- At present, the HIFI pipeline produces Level 2 spectra with frequency axis in the LSR frame, including Solar System Objects (SSOs). SSO spectra should be presented in their rest frame.

10.2 Absolute Frequency Consistency

Literature velocities have been compared with a set of HIFI line measurements, and in all cases found good agreement given the uncertainties (e.g. different species, data S/N ratios). An example shown below is CO 6-5 in IK Tau, in which the measured velocity shift is in excellent agreement with the intrinsic source velocity.

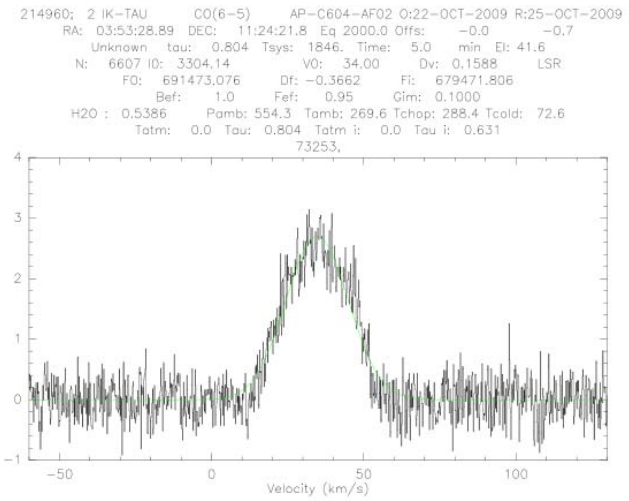

Figure 27: CO 6-5 in NML Tau (IK Tau), with a measured velocity shift of 34.0 km/s that agrees with the intrinsic velocity of the source, and with APEX measurements.

When possible, a cross-comparison between modes and a check of the spectral line repeatability has been made, e.g. using the CO 5-4 line towards o Ceti, also observed from ground by APEX. Agreement between H and V and both spectrometers HRS and WBS has been verified, in terms of line centre frequency and FWHM. Agreement in nominal, except for the centring of the line within the HRS frequency bandwidth because of a difference in computing and adjusting the sub-band placement for the spacecraft velocity, in different reference frames (LSR vs SSB). A solution to this problem is under investigation; meanwhile the effects

are significant only for the HRS when used in high resolution mode in the high frequency bands.

10.3 Multi-epoch Frequency Consistency

Observations of the same line and source at multiple epochs have also been compared, and the detected line frequencies match. The longest check was for sourceLDN1157- B1, taken 186 days apart, and the motion of the spacecraft is correctly removed to an accuracy of better than 0.5 MHz (0.3km/s). A detailed summary of H and V profile agreement is given in Sec. 11.

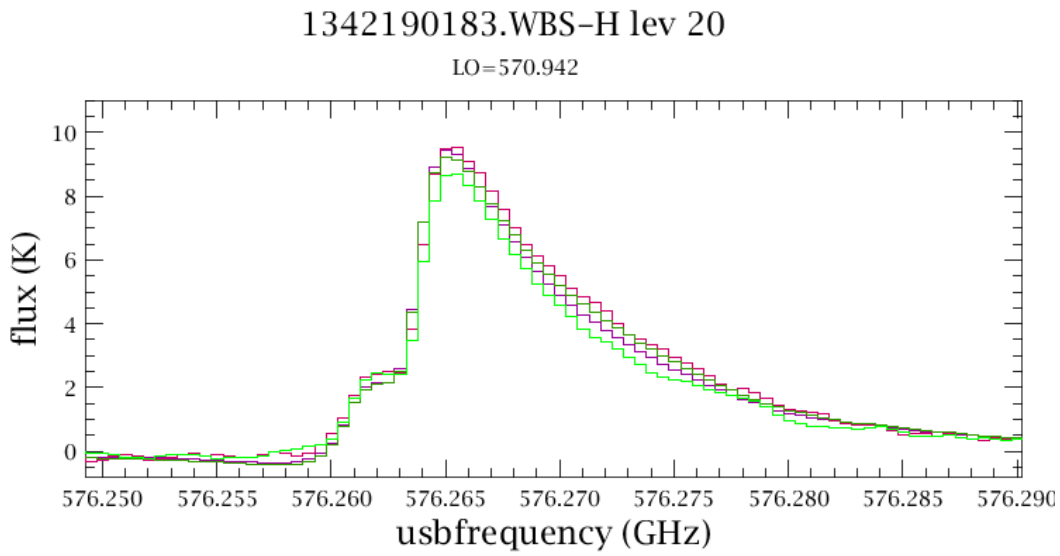

10.4 Solar System Objects

Observations of Comet Wild-2 were checked against the predictions of the Horizons ephemeris. The Herschel-centric, Wild-2 apparent radial velocities were queried and interpolated to the time of observation.

The Level 2 frequency axis is affected by the issues listed above; but within HIPE one can easily use Horizons to predict the IF frequency of detection, using an appropriate spacecraft ephemeris (H20090622_0001.LOE). The water lines are found to be within at most 0.5 MHz of the predicted frequency (see the table below). Whether the differences between HRS and WBS are significant is still being investigated.

H20 1(1,0)-1(0,1) 556936.00 MHz

Backend	pred-detect (IF)(MHz)
WBS-H	-0.07
WBS-V	0.03
HRS-H	0.33

HRS-V	0.33

H20 1(1,1)-0(0,0) 1113342.96 MHz

Backend	pred-detect (IF)(MHz)
WBS-H	0.11
WBS-V	0.41
HRS-H	0.51
HRS-V	0.51

Example Wild-2 spectra (Level 1) are below. Note that the negative amplitudes are a result of the ON an OFF phases being out of synchronization in the pipeline after timing-related command completion errors in the FastDBSCross mode. The Level 2 frequency scale below is in the LSR frame.

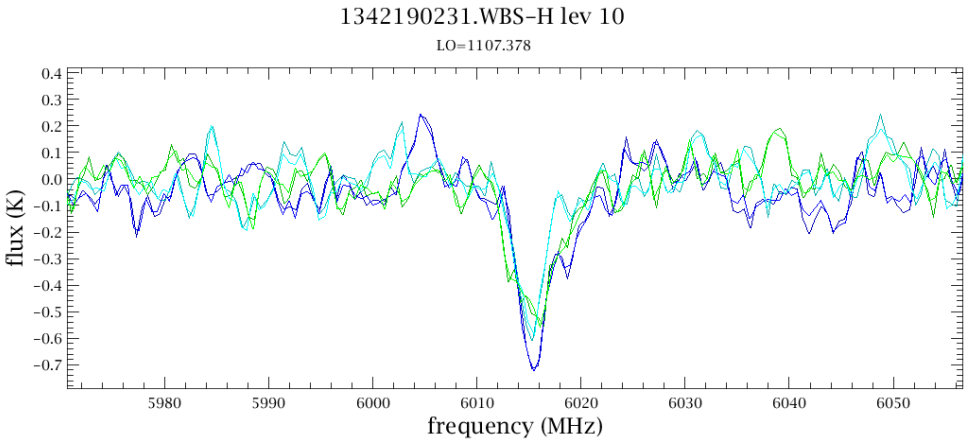

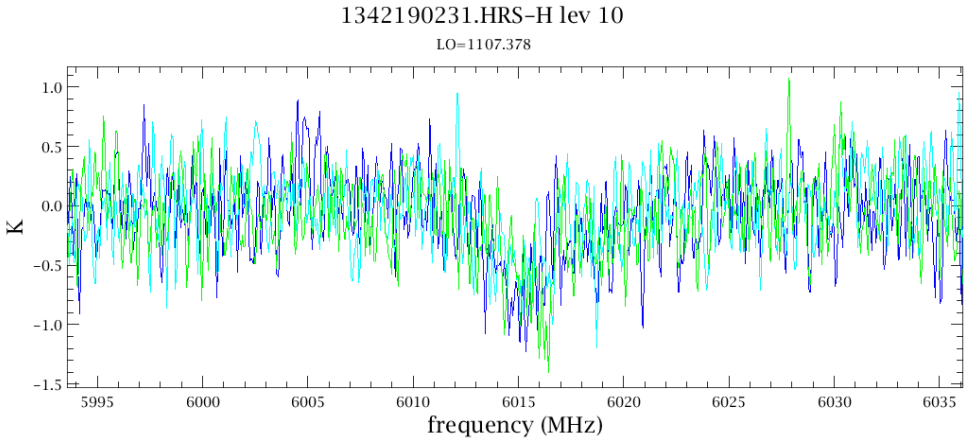

10.5 Velocities in the HIFI Observation Context

For the interest of the User, here is summary of the several velocities one can find in the metadata and data in the Observation Context. This discussion applies to HCSS 2.0.1453. They will change in the near future.

a. obscon.meta['radialVelocity'] : opposite of V_lsr.
   This is the velocity of the spacecraft, as seen by an observer at rest in the LSR, in the direction of the target. This may not be actually used for anything in the pipeline (TBC), rather (c) below is used in computation.

b. htp.meta['vlsr'] :
   This is the User-entered redshift from HSPOT, used in setting the LO in uplink so that the desired line is in the band, but has no other explicit role in the pipeline at present. In the near future it will be used to transform spectra to the rest frame of the target.

c. dataset['velocity'] column:
   Same as (a), but for the particular time and pointing of the spectrum.

11. H and V Profiles

11.1 Contributing sources of H and V profile disagreements

The agreement between H and V profiles of lines observed during PV has been investigated, with particular attention paid to an outflow source, L1157-B1, which was originally observed during PV-1 in August 2009 and exhibited a deviation between the H and V line intensities of up to 20% and re-observed twice during PV-2. The levels of agreement (or disagreement) are important to characterize, since contributing factors may include any of telescope pointing, angular separation of the H and V beams on the sky (cf. Sec. 8.3 and the table below), possible intrinsic polarization of the source at the line frequencies of interest, and instrument calibrations (different beam efficiencies or sideband gains) or power level output from the spectrometer back-ends. The internal calibrations could account for up to 6-8% disagreement between H and V profiles, measured as integrated fluxes.

IF spectral repeatability of point sources (see Sec. 12) show that H and V profiles are in good agreement across bands 1, 2, 4 and 5 to within 3%. The beam efficiencies will be more fully characterised after observations of Mars in April 2010.

The effect of pointing offsets between the two polarisations on line profiles in the case that the emission is extended or has a strongly varying velocity structure is harder to quantify. The difference in H and V co-alignment was measured during the Check-Out Phase and the findings are given in the Table below.

Band	ΔHV in Y (“)	ΔHV in Z (“)
1	-6.2	+2.2
2	-4.4	-1.3
3	-5.2	-3.5
4	-1.2	-3.3
5	0.0	+2.8
6	+0.7	+0.3
7	0.0	-1.0

Table 5: Co-alignment of H and V beams as measured during CoP.

11.2 Compact Sources

Line centres and line shapes are in excellent agreement between H and V profile among the AGB stars observed during PV-2. In many cases, the V polarisation shows the stronger line but typically the peak values of the H profiles fall within 7% of the peak in V.

One exception to this is NML Tau, which showed differences in the peaks of profiles of over 30%, in some cases. Some of the profile discrepancies (e.g., obsid 1342190160 where the peak of the V profile was 1.275 times that of the H) can be attributed to data quality that suffers from when the line is located at the band edge in a region of high Tsys (see Sec. 6). In two other cases it was found that there was a greater scatter of individual datasets at Level 1 about the mean in one polarisation (V) than the other (see Figure 28 below), possibly reflecting different power output levels between H and V.

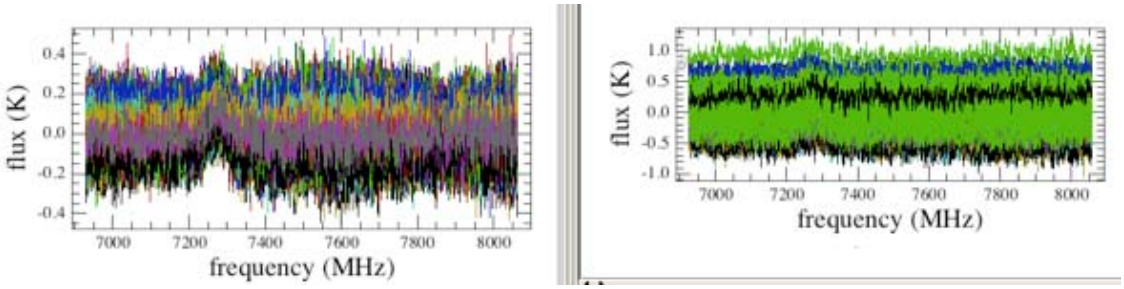

Figure 28: The spread in datasets at Level 1 in V (right) is three times that of H (left), this contributed to a 22% difference in the peaks of the H and V Level 2 profiles in obsid 1342190160.

In certain cases this effect at Level 1 leads to an apparent shift in line centre in the V polarisation at Level 2, but this could be remedied by removing outlier scans from the Level 1 data before averaging.

Beyond these cases, there remains a larger difference in H and V profiles than is expected from uncertainties in sideband gain or beam efficiency correction. In the spectrum below of NML Tau the peak in H is 74% of that in the V polarisation.

After simply scaling the H polarisation up it is seen that there is no mismatch in profile shape.

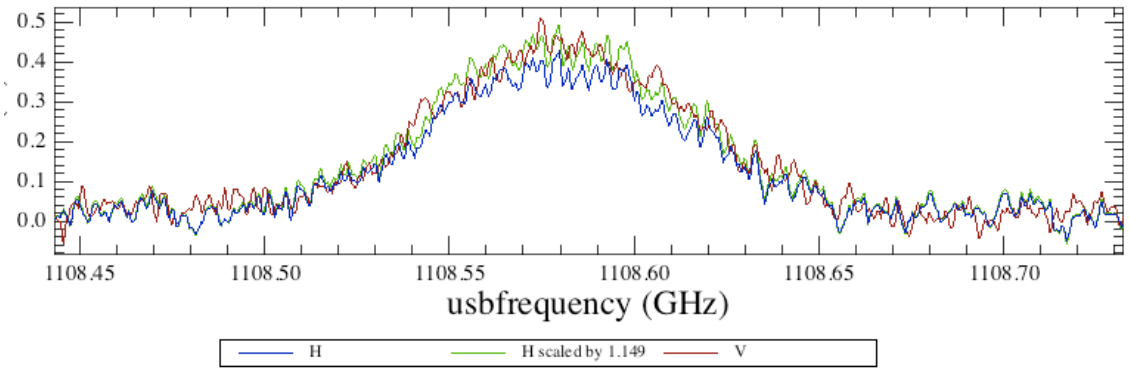

Figure 29: H and V profiles in this observation differ by 26% at the peak, rescaling so the peaks match show no difference in line shape

11.3 Extended Sources: LDN1157-B1 in detail

L1157 is a well-known Class 0 proto-star associated with an energetic outflow that displays shocked structures along its length including a bow shock in the blue lobe. The velocity structure around the source is also complicated by in falling and accreting material.

Observations in the blue lobe of L1157 were made in Band 1b in Spectral Scan DBS mode with (1342181161) and without (13421811160) continuum optimization during PV-1 in August 2009. The two observations were well matched with each other but displayed a pronounced discrepancy in CO 5-4 H and V profiles reaching up to 20% in the line wings. The profile discrepancy was still seen even after the peak in the H polarisation was scaled up to align with that in V profile, with the V remaining stronger in the wing.

L1157-B1 was observed again in Band 1b 186 days later in PV-2, using the PointFastDBS mode with continuum optimization (1342190183) and in PointDBS without continuum optimisation (1342190184), and the latter observation repeated again in the same 40 days later (1342192229). The roll angle of the telescope is ~180° with respect to the PV-1 observations. In all cases the V polarisation displays a higher intensity line than the H. Figure 30 shows the H and V line profiles for observations 1342181160 (160), 1342190184 (184), and 1342192229 (229), scaled so that all the peaks (per observation and polarisation) align.

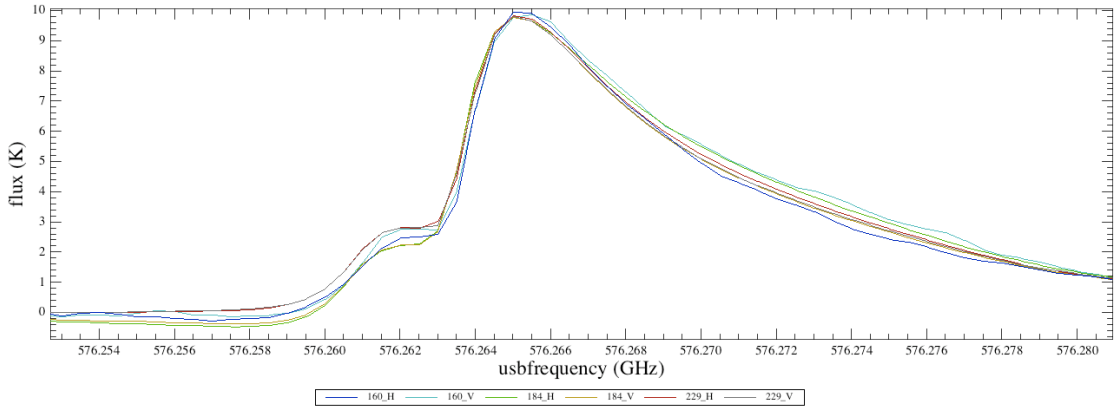

Figure 30: H and V profiles for obsids1342181160, 1342190184, and 1342192229, scaled so line peaks match.

There are several things to note from this figure:

- The polarisation discrepancy in the wing is in the opposite sense for 160 and 184.
  - As the observations were performed 6 months apart, this could imply that there is some bright region of the outflow contributing to the profile mismatch rather than an intrinsic polarisation effect.
- It can be seen that the profile discrepancy has reduced with successive observations from approaching 30% in 160, to 10% in 184, until in 229 there is a difference in profile in the wing of only 4% (Figure 31).
  - 184 has a lower noise goal resolution than 160, while 229 is free from emission in chop positions.

The discrepancy at the peak of the line is very similar for 160 and 229, and is approximately 8% but is only ~4% for 184. This could be an effect of the emission in the chop position (see next bullet).

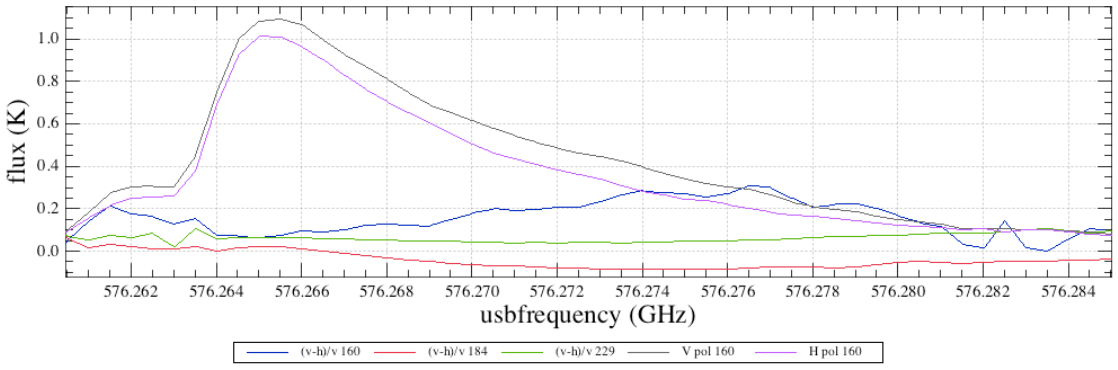

Figure 31: Fractional differences in H and V profiles approach 30% (160), 10% (184) and 4% (229). The H and V profiles of 160 are plotted to illustrate the variation across the line.

- There is a clear dip before the line peak in 184 (also seen in 1342190183) and a hint of the same in 160.
  - Investigation of the reference positions at Level 1 show that there is emission in the reference position when chopping off the source for 184 (Figure 32).
  - There is no emission is the reference positions for 229.
  - The H and V profiles in 184 and 160 show some discrepancy at frequencies below the line shift, while 229 does not, this effect is due to the emission in the chop position.
  - The contaminating emission does not affect the line profiles in the wing. There is no evidence of differing levels of emission in the two reference positions, but this does not preclude the possibility that both reference positions contain an equal level of emission. However, this shows that the differences in profile in the wing are not a product of chopping into source.

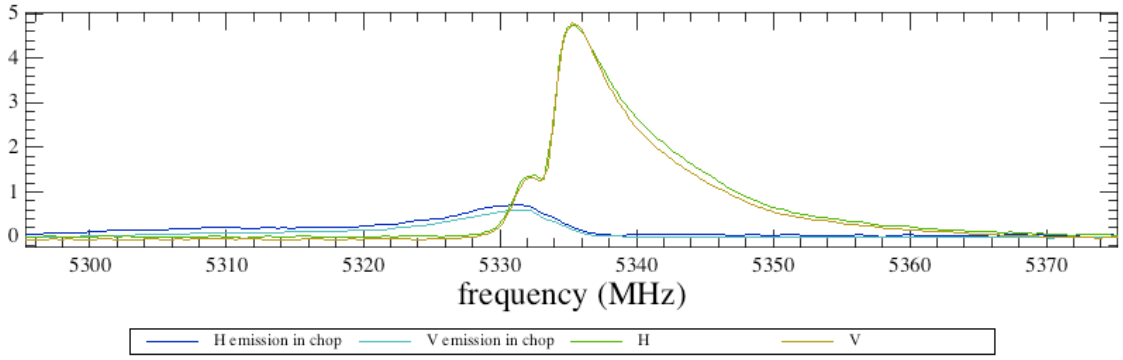

Figure 32: 1342190184. Emission in chop position from On source. The contaminating emission affects the line profile until just beyond the peak, and so has no influence on the discrepant H and V profiles in the wing.

From the above, an investigation of the separate emission in the reference positions and ON source is warranted. To do so, the observations were reprocessed, skipping the doRefSubtract and doOffSubtract steps of the Level 1 pipeline (using HIPE 2.6). The reference and source measurements could then be investigated in the ON and OFF positions. Figures Figure *33*Figure 34 show the H and V profiles derived from the ON and OFF positions separately for 184 and 229, respectively. A profile difference can be seen even in one polarisation between the two positions.

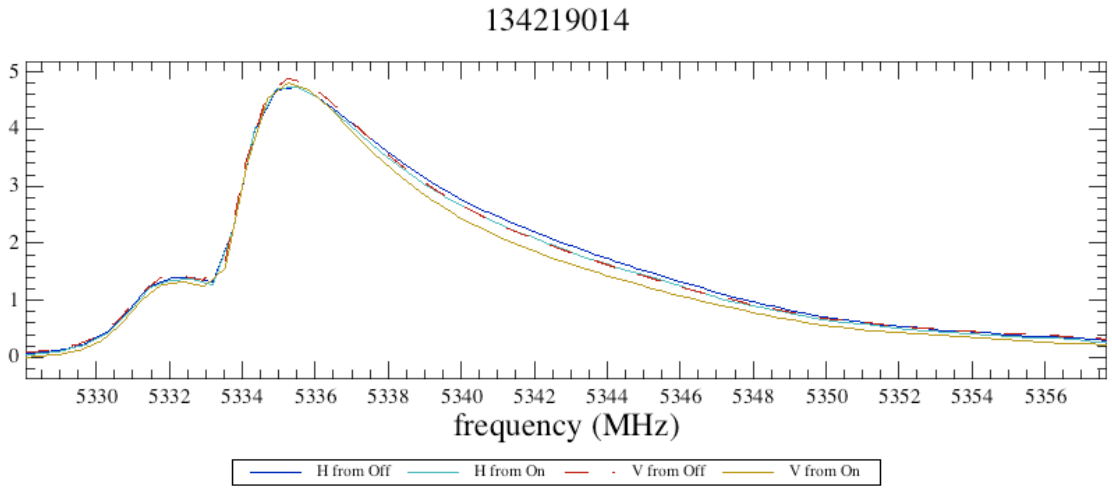

Figure 33: H and V profiles derived from ON and OFF positions separately for 1342190184. It is interesting to note that the V profile from the OFF position corresponds exactly with the H profile from the ON position.

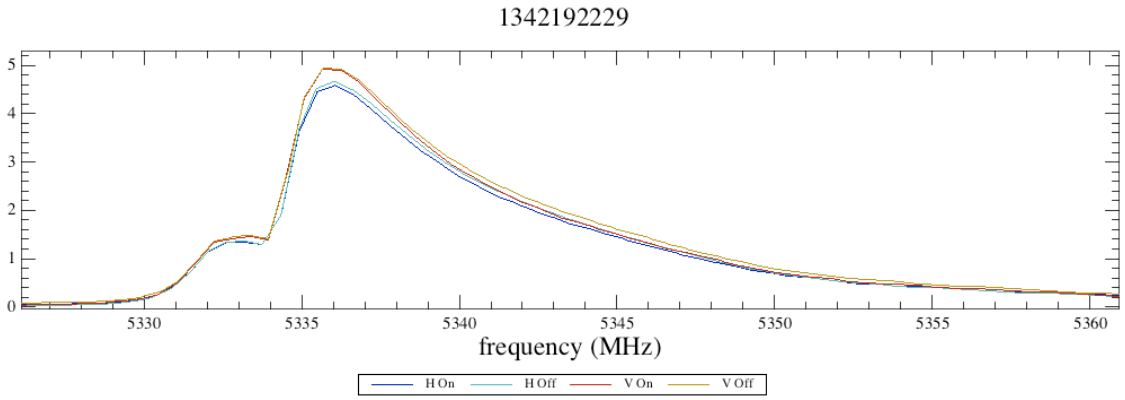

Figure 34: As for HV-6 but for 1342192229. The same behaviour is seen but the overall spread in profiles is smaller than for 184.

One possible reason for this behaviour could be that there is some scatter in where HIFI points for each integration due to shifts after telescope slews between the ON and OFF positions and as HIFI chops between source and reference. Figure 35 shows the pointings for each integration on source for 184, the spread is approx 2" (and is very similar for 229).

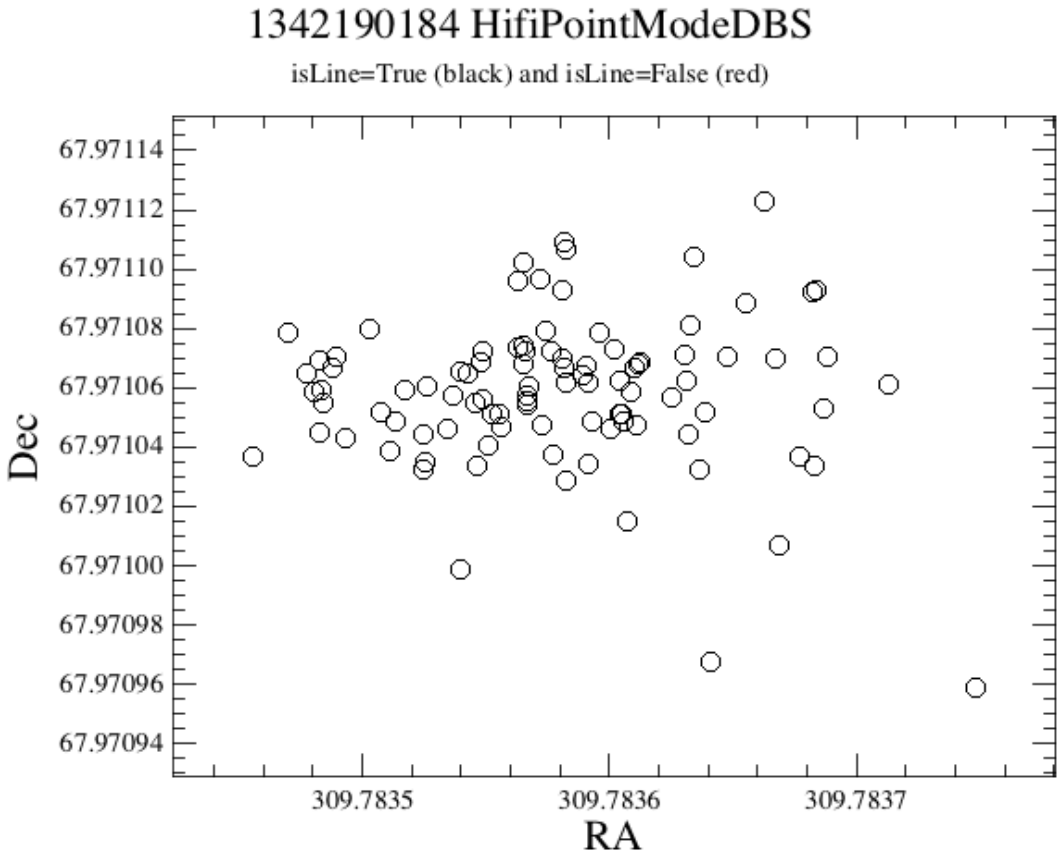

Figure 35: Pointings of each integration on source for 184.

This scatter in pointing (and perhaps in combination with velocity structures arising in shocked regions in outflows) could give rise to the difference in profiles seen between the ON and OFF positions. In support of this theory, the fractional difference in intensity relative to the mean intensity of each integration for each polarisation are plotted in Figures Figure *36*, Figure *37*, and Figure *38* for the ON and OFF positions. A line profile is plotted in each case to show variation with position in the line. If variations between individual integrations are affecting the profile in the wing then the fractional difference should increase there.

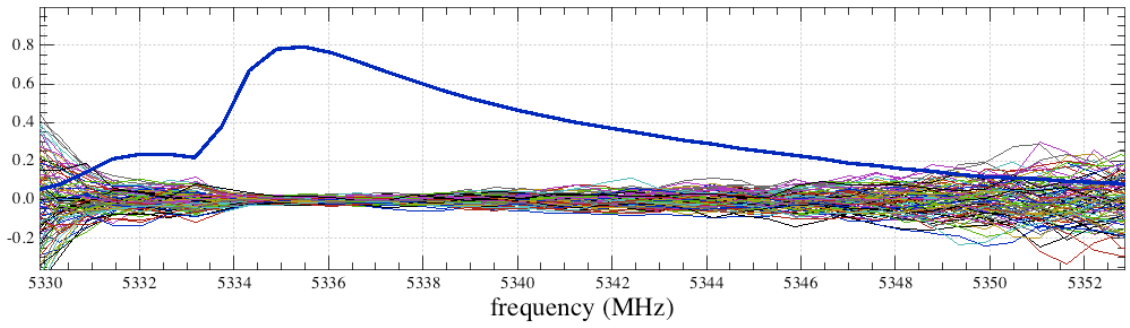

Figure 36: (H-Hav)/Hav for the Off position for 1342190184.

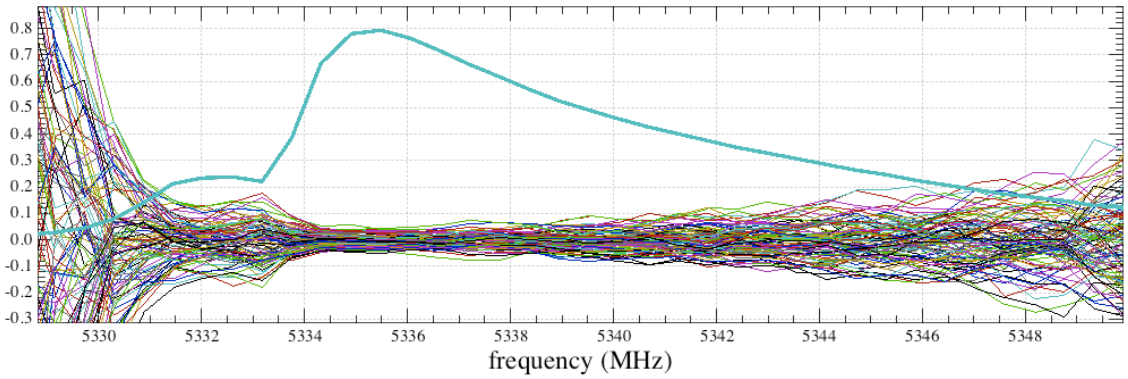

Figure 37: (H-Hav)/Hav for the On position for 1342190184. The spread is greater at the low frequency end of the line than for the Off position, this may be due to the emission in the chop position.

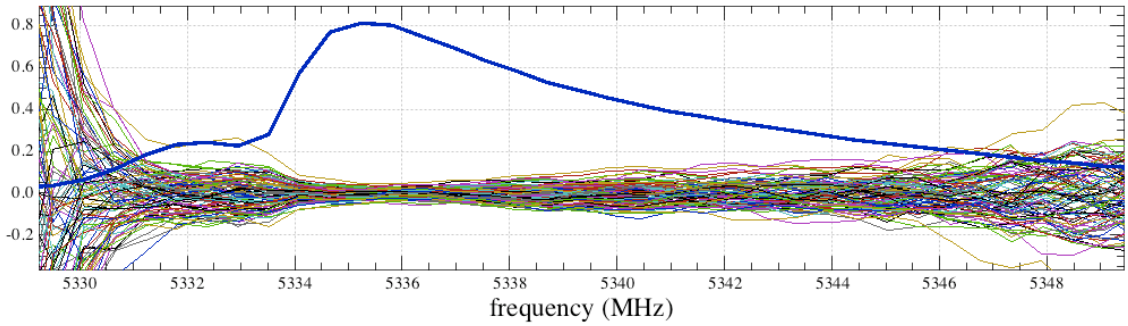

Figure 38: (V-Vav)/Vav for the ON position for 1342190184.

The fractional difference reaches (and even exceeds) 0.1 in the wing of the profile, compared with <0.05 near the line peak. In band 1 the offset between the H and V beams is (-6.2", 2.2"). It seems reasonable that if a scatter in pointings can give rise to a difference in one polarisation between ON and OFF positions then this further difference in pointing in H and V could cause differences in H and V profiles. Furthermore, if the chop direction was along the outflow, as was the case for 160 and 184 this could generate a significant difference in H and V in the wing of the profile.

11.4 Summary and Conclusions

- Comparison of H and V profiles in compact sources show that the line profiles agree to within 7%, which is within current calibration uncertainties.
    - An exception to this is NML Tau, which shows deviations of up to 30%

    - Some of these discrepancies were found to be due to issues with the data such as poor line placement or scatter in data at Level 1
- It is harder to disentangle the effects of extended emission and pointing offsets between the H and V beams.
    - Artificial polarisation effects can be created due to the H and V beam offset and can be particularly affected in if there is a strong velocity structure associated with the observation.
    - In the case that polarisation differences are of importance, care should be taken to avoid chopping into emission.
- When investigating differences in H and V profiles, it is helpful to go back to Level 1 data.

12. IF Spectrum Repeatability (Sideband Line Ratios)

Specific tests have been carried out in the laboratory and on-orbit since the first checkout phase and again during CoP-II and PV-II, to assess the repeatability of spectral lines occurring at different IF frequencies in both upper and lower sidebands. On orbit these tests have been done so far in beam splitter Bands 1b, 2a, and 5a, and diplexer Band 4a, towards NGC7538 IRS 1 using the strong CO lines. The frequency was gradually changed so the line was stepped across the band to look for changes in intensity. Figure 39 shows how this looks in the Band 1b engineering test, with all 15 spectra of the same CO 5-4 line over-plotted in IF frequency in the upper sideband of the WBS-V. Figure 40 shows a similar example, taken from a different source using a standard Spectral Scan in 1b on the H_2O $1_{10} – 1_{01}$ 557 GHz line.

All of the tests were done in DBS mode. The line signal is typically 10-20K and noise less than 0.2K, resulting in a S/N ratio of over 100.

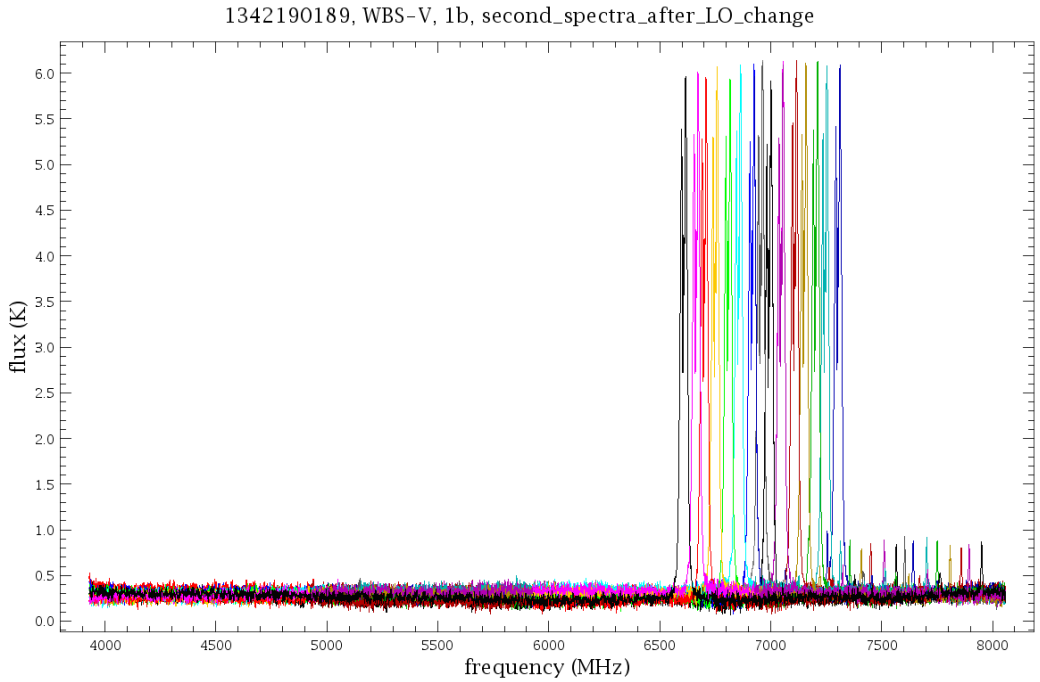

Figure 39: CO 5-4 with WBS-V, spaced across the upper sideband from an engineering Spectral Scan.

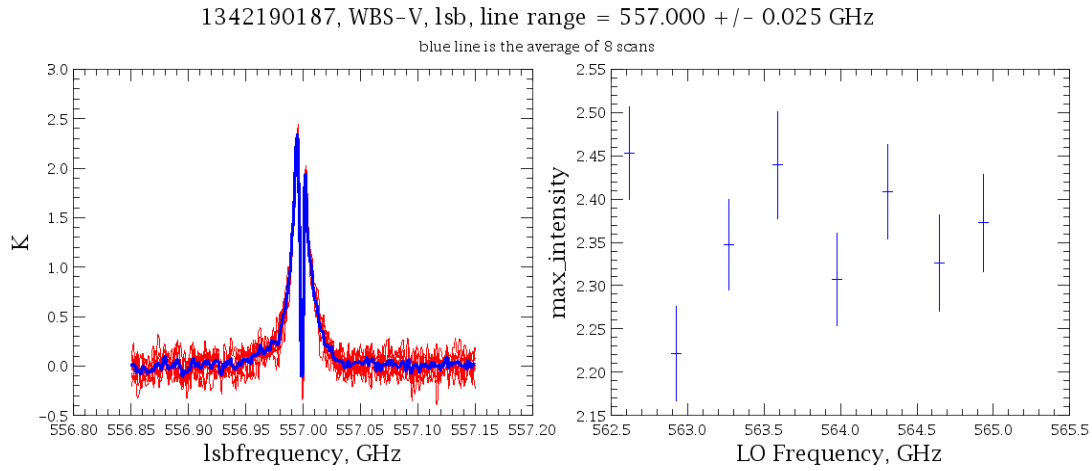

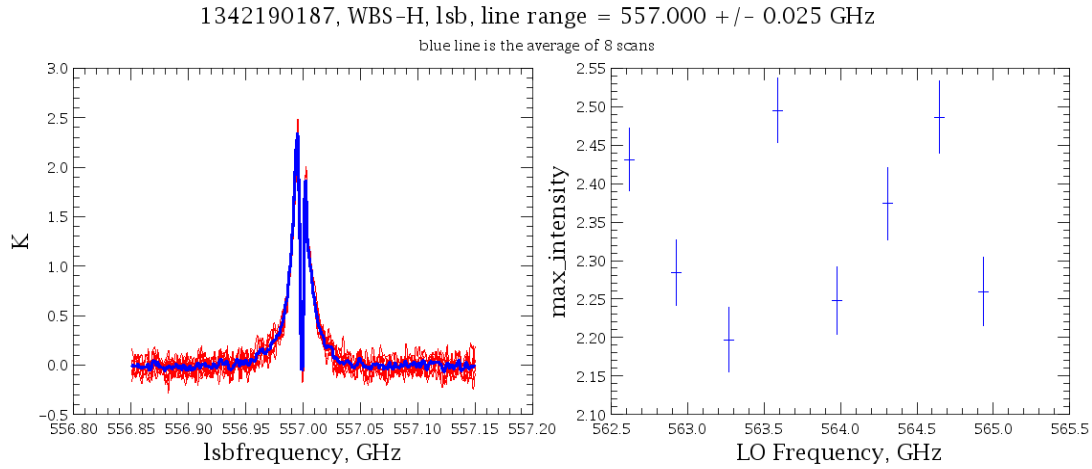

Figure 40: Measurements of the 557 GHz water line at 8 positions in the LSB in WBS-V (upper) and WBS-H (lower).

While the comparison between flight data and ground-based gas cell measurements is ongoing, the following conclusions are reached for the bands without diplexers:

- **Band 2a**: the integrated line intensities vary by less than 1% around the average value.

- **Band 5a**: there is a slight USB/LSB line strength difference (3%). This is true for both polarizations. The (H-V)/H intensity difference is also 3% on average; true for both sidebands. This could be due to pointing offsets between the polarizations.

- **Band 1b**: similar to Band 2a.

For **Band 4a**, the only diplexer band tested so far, the SBR test was carried out without retuning the diplexer, and then the same test was redone but with retuning. The conclusions are reached:

1. The observations *without* diplexer retuning show that in the unlikely event of a diplexer mistune, the diplexer window significantly affects calibration. At least some of this variation can be eliminated by recalibrating with the ratio of the noise levels at the frequency for which the diplexer is correctly tuned. This should not happen for normal observing.

2. The Standing Wave test showed no convincing effect -- the variation is less than \pm 2% and this slight variation does not show a 650MHz period like the diplexer standing wave.

3. With the diplexer retune, and only taking into account the scans preceding the sharp increase in noise level, the CO 9-8 line seen in the LSB is a few

percent weaker than in the USB. It remains to be seen if this is a real SBR effect or rather due to the diplexer. All of the variations seen are greater than identical spectra affected only by random noise at the RMS noise level.

4. The V polarization is systematically stronger than the H but the line profiles are different (see Figure 41), suggesting that at least part of the difference is due to a pointing offset.

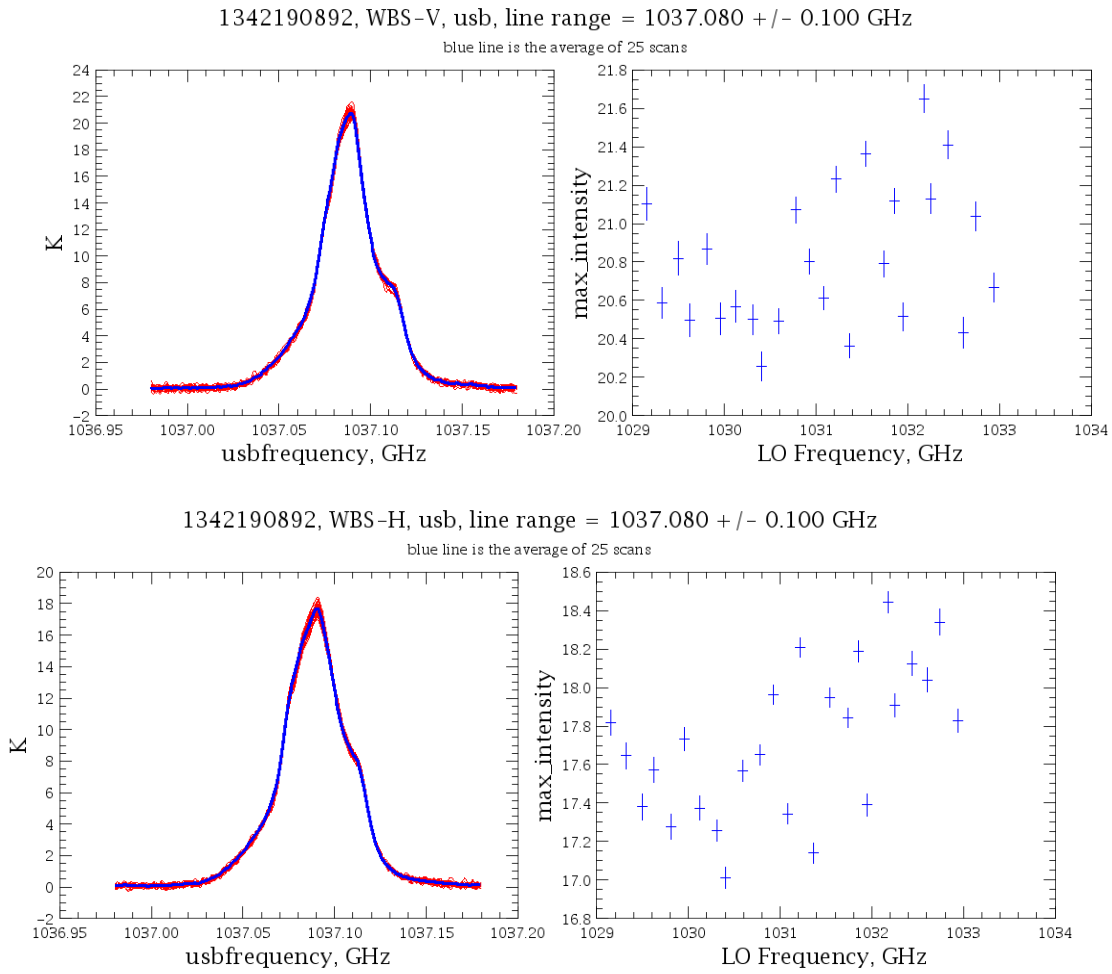

Figure 41: Measurements of the 1037 GHz CO 9-8 line at 25 positions in the USB in WBS-V (upper) and WBS-H (lower).

5. The RMS noise was much greater when the CO line was in the LSB (high LO frequency) and this was true for both polarizations.

A summary of these results is represented in Figure 42.

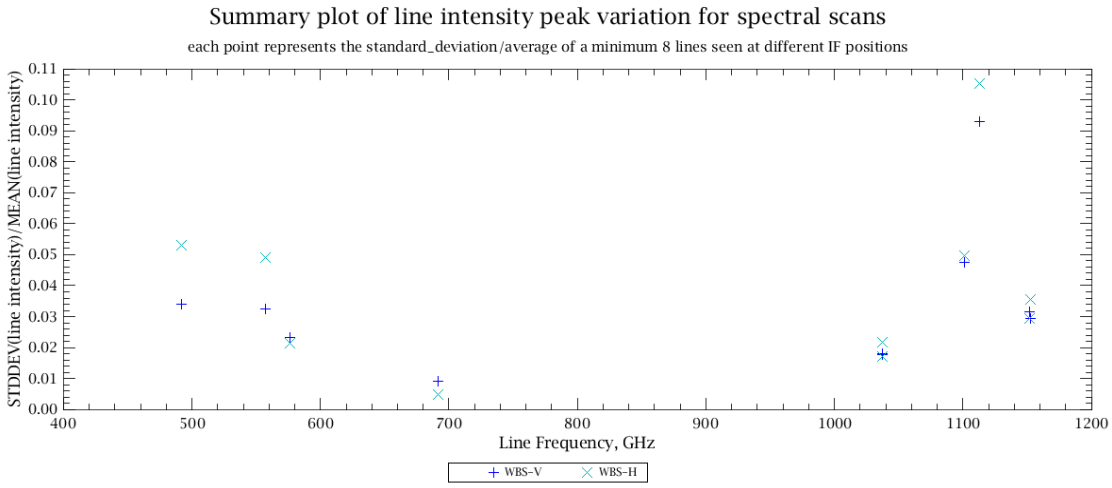

Figure 42: Peak intensity variation of spectral lines as measured at 8 or more positions in the IF, from PV-II Spectral Scans.

13. Spurious Responses in HIFI

HIFI, like all heterodyne receivers, suffers from spurious response. These 'spurs' can significantly degrade the quality of spectra, and therefore it has been prudent to track and catalog these features in all HIFI data taken since pre-launch. This catalog has been implemented in HSPOT so Users can be warned if they tune the LO near the position of known spurs.

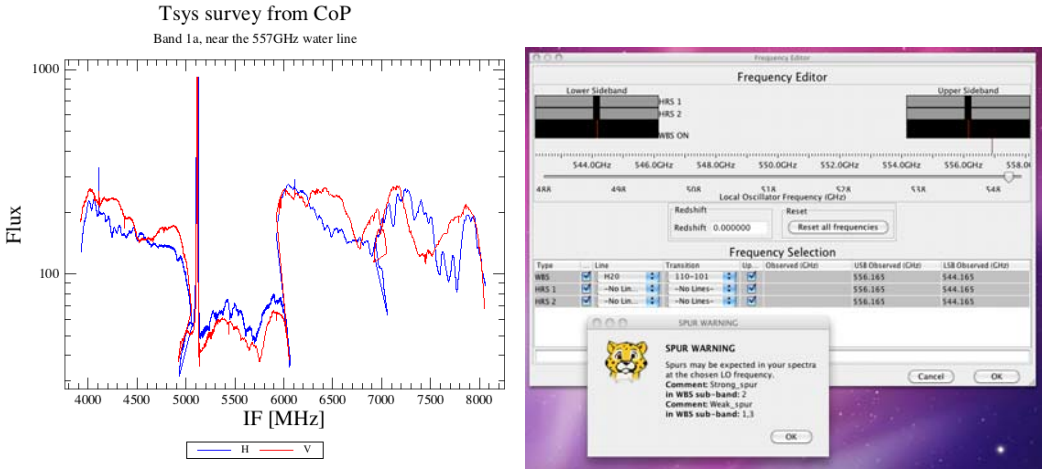

Figure 43: On the left is the spectrum from the CoP Tsys survey related to the HSPOT AOT on the right. Weak spurs are seen in the first and third WBS subband, and a strong spur, which in addition to saturating the detector, suppresses the flux from the entire subband. In the HSPOT window, the User placed the desired water line in the third subband of the upper sideband, and the system generated a warning. In this particular case, the weak spur poses no threat to the line.

13.1 Analysis of spurious responses in WBS

In general spur positions and strengths have remained similar between the prime and redundant sides, and across over a year of data acquisition stretching back to pre-launch test activities.

The spurs that cause the most concern are the ones near important water lines.

13.2 Spurs in Band 1a

In 1a, a strong spur exists blueward of 548.7 GHz. This spur is very strong, saturating the detector and rendering the entire 4GHz passband unusable. This is unfortunate, as it directly impacts observations of the 557 GHz water line. There are very narrow (~500MHz) regions in LO tunings where the spur seems well behaved and one could in principal take a relatively clean spectrum. However it is not clear how stable this 'safe zone' is over time. We recommend that Users try to use the lower sideband of band 1b if possible.
Note that engineering tests in PV revealed that it may be possible to remove the spur by making slight changes to bias settings on the receiver. This will be tested, and if successful, we can modify our recommendations for this band.

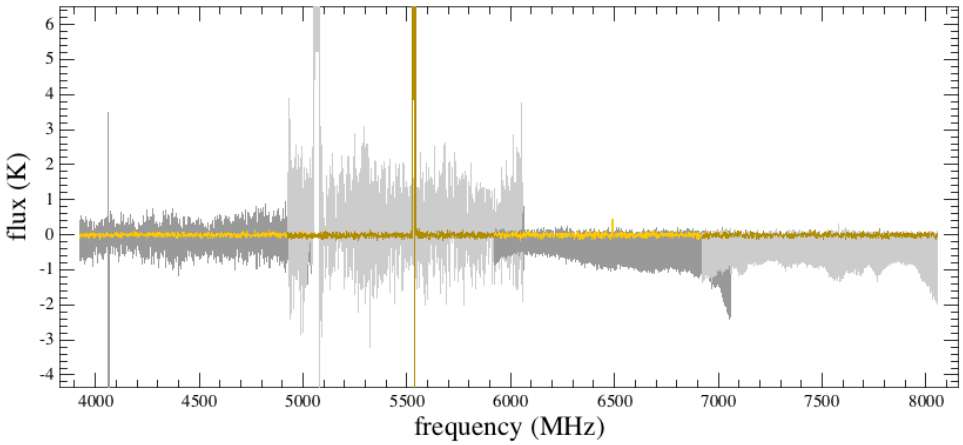

Figure 44: Spectra taken from 2 different LO tunings in 1a. The grey plot is from a tuning of 549.3 GHz and the spur wipes out not only the subband in which it resides (2), but the entire spectra due to the crosstalk. At 550.4 GHz however (yellow trace), the spectrum is well behaved aside from the spur in the second subband.

13.3 Spurs in Band 4b

Water at 1113 GHz is potentially corrupted by a spur that appears between LO tunings of 1090 GHz and 1108 GHz. However unlike the 1a spur, this one is very weak and sometimes disappears altogether, likely due to changes in instrument temperature.
It is still recommended to place this spur in a subband different from that of the water line. The position of the spur in the IF as a function of LO is fit well by the following formula:

$$IF = 5064.9 - 44.3x - 0.6x^2$$

where $x = LO - 1090.498$ GHz

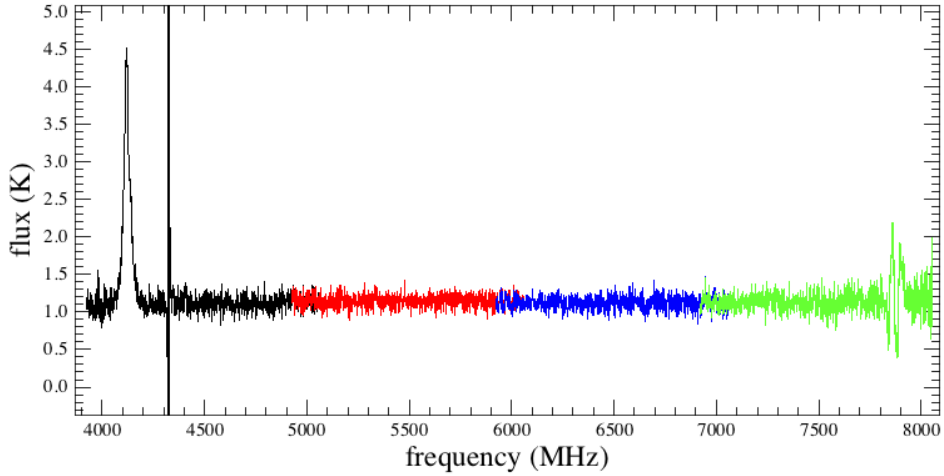

Figure 45: Though band 4b spurs are strong compared to real lines, they are very narrow and do not seem to affect the integrity of the spectra around them. This spectra was taken during PV at an LO setting of 1105.6 GHz.

13.4 Spurs across other bands

A detailed analysis of spurs is ongoing based on observations taken in PV. A summary of the table that HSPOT uses is provided here. Users who need LO tunings in any of the affected ranges are encouraged to contact the helpdesk(s) for advice.

Note that the ranges could be as much as 2GHz wider on each side of a spur due to the resolution of the surveys from which these were determined.

- **Band 1a**: Strong spur above 548.7 GHz.
- **Band 1b**: No spur activity.
- **Band 2a**: Spurs at 700.0 GHz, and 712.0-718.0 GHz.
- **Band 2b**: Spurs at 772.0 GHz, and 776.0-788.0 GHz.
- **Band 3a**: Spur at 823.0 GHz.
- **Band 3b**: Spurs between 868.0 – 876.0 GHz, and 952.0-954.0 GHz.
- **Band 4a**: Spur at 967.0 GHz, and 1001.0-1003.0 GHz, and 1017.0 GHz.
- **Band 4b**: Spur between 1090-1108 GHz.
- **Band 5a**: Spurs between 1232.0-1240.0 GHz
- **Band 5b**: Spurs between 1232.0-1236.0 GHz, 1258.0-1272.0 GHz.
- **Band 6a**: Spur at 1544.0 GHz
- **Band 6b/7a/7b**: No conclusions yet.

13.5 Spurious response in HRS

Spurs in WBS do not correspond to spurs in HRS. While the investigation of HRS spurs has not yet been as detailed as in WBS, it is already clear that the spur in 1a for instance does not impact the HRS at all. Because spurs are found

generally in spectral surveys, and since spectral surveys generally do not have HRS data, a full catalog of HRS spurs has been slower to generate.

13.6 Treating spurs in software

Spurs are automatically flagged during pipeline processing, and ignored in subsequent processing. For moderate spurs, this is generally sufficient. Strong spurs however, which corrupt entire subbands or spectra, require an extra step of cleaning.
This is easy to do in software, and we have had excellent success in cleaning up spectral scans for use by the deconvolution.

14. HIFI intensity calibration budget

The following table summarizes the relevant parameters and effects and our current knowledge and strategy.

Parameter	Status	Strategy	Next action
Beam efficiencies	Parameters known based on theoretical modelling; preliminary values derived from Saturn observations; accuray 5-10%	Use theoretical values until measured	Observations in April 2010 on Mars
Coupling coefficients	Measured in ILT, no further change expected; accuracy 3-5%	Leave as is	
Chopper position HBB/CBB		Treat as error	
Standing waves towards calibration loads		Treat as error	Can be modelled?
Sideband ratio	Analysis of gas-cell measurements from ILT; accuracy is a few percent for beam-splitter bands, up to 20% for diplexer bands.		Diplexer modelling
Standing waves	HEB IF standing wave analysis ongoing, effect on accuracy TBD		Tests during PV-II
Continuum linearity			
Line linearity	Negligible error		
Pointing	first FPG-3 done during PV	Continue to monitor	Dedicated observations in April 2010 on Mars
Spurs	Inventory of spurs available, Hspot assists with avoiding		dedicated program for spurs in selected

	most critical frequency areas		bands
IF feedback	Expected to be mostly negligible	treat as error until sufficient data available to allow correction	evaluate measurements done in PV-II

15. Appendix

15.1 dumpHIFIsiam.py

```
from herschel.pointing.siam import SiamReader

import string
import math

mySIAM = "/your/path/to/nnnn_mmmm.SIAM"
# example: mySIAM = "/home/michael/HIFI/pointing/0068_0002.SIAM"

HifiApertures = (
    "H11_0", "H12_0", "H13_0", "H14_0", "H15_0", "H16_0", "H17_0", "H18_0",
    "H21_0", "H22_0", "H23_0", "H24_0", "H25_0", "H26_0", "H27_0", "H28_0",
    "H31_0", "H32_0", "H33_0", "H34_0", "H35_0", "H36_0", "H37_0", "H38_0",
    "H41_0", "H42_0", "H43_0", "H44_0", "H45_0", "H46_0", "H47_0", "H48_0",
    "H51_0", "H52_0", "H53_0", "H54_0", "H55_0", "H56_0", "H57_0", "H58_0",
    "H61_0", "H62_0", "H63_0", "H64_0", "H65_0", "H66_0", "H67_0", "H68_0",
    "H71_0", "H72_0", "H73_0", "H74_0", "H75_0", "H76_0", "H77_0", "H78_0")

csvfile = string.replace(mySIAM, ".SIAM", ".csv")
csv = open(csvfile, "w")

sr = SiamReader(mySIAM)
print sr.siamVersion
csv.write('"instrument","aperture","X","Y","Z"\n')

R2S = 3600.0*180.0/math.pi
for aper in HifiApertures:
    siam = sr.getSiam(aper)
    theta = siam.toEulerZYX().negate()
    x = theta.x
    y = theta.y
    z = theta.z
    if z < -math.pi:
        z = z+2.0*math.pi
    x = x*R2S
    y = y*R2S
    z = z*R2S
    csv.write('"HIFI","%s",%20.15e,%20.15e,%20.15e\n' % (aper, x, y, z))
    print "HIFI  %s %20.15e %20.15e %20.15e" %  (aper, x, y, z)

csv.close()
```